Soluble LAG-3 Identifies a Dynamic Early T Cell Activation Window in self-reactivity, Type 1 Diabetes, and Broader Immune Responses.

Saptarshi Roy[1,2,*,a], Megan L. Proffer[2,10,a], Farooq Syed [3,4], Megan E. Smithmyer[5], Avinil Das Sharma[2,6,9], Abigail Twoy[7,8], Emily Soo-Hoo[7,8], Jyoti Rana[3], Jason M. Spaeth[2,6,9], Everett Meyer[7,8], Kent P Jensen[7,8], Cate Speake[5], William Hagopian[2,6], Jon D. Piganelli[1,2,10*]

1. Department of Endocrinology, Indiana University School of Medicine, Indianapolis, IN, USA.
2. Center for Diabetes and Metabolic Diseases, Indiana University School of Medicine, Indianapolis, IN, USA.
3. Department of Diabetes-Immunology, Arthur-Riggs Diabetes and Metabolism Research Institute, Beckman Research Institute at the City of Hope, Duarte, CA, USA.
4. Center for RNA Biology and Therapeutics, Beckman Research Institute at the City of Hope, Duarte, CA, USA
5. Center for Interventional Immunology, Benaroya Research Institute, Seattle, WA, USA.
6. Department of Pediatrics, Indiana University School of Medicine, Indianapolis, IN, USA.
7. Division of Blood & Marrow Transplant & Cell Therapy (BMT-CT), Stanford University School of Medicine, Stanford, CA.
8. Diabetes Immune Monitoring Core (DIMC), Stanford Diabetes Research Center (SDRC), Stanford University School of Medicine, Stanford, CA.
9. Department of Biochemistry and Molecular Biology, Indiana University School of Medicine, Indianapolis, IN, USA.
10. Department of Microbiology and Immunology, Indiana University School of Medicine, Indianapolis, IN, USA.

***Corresponding Authors:**

***Jon D. Piganelli**, PhD, Department of Endocrinology, Indiana University School of Medicine 1210 Waterway, 4th floor, 4100F, Indianapolis, IN 46202. Email: jdpigane@iu.edu, Phone: 317-278-6013

***Saptarshi Roy**, PhD, Department of Endocrinology, Indiana University School of Medicine 1210 Waterway, 4th floor, 41007, Indianapolis, IN 46202. Email: roysapt@iu.edu , Phone: 317-278-6013

[a] Both authors equally contribute.

Abstract

Aims/hypothesis: Type 1 diabetes is a complex autoimmune disorder in which autoreactive $CD4^+$ and $CD8^+$ T cells destroy pancreatic beta-cells, resulting in insulin deficiency and hyperglycemia. Although genetic susceptibility, particularly certain HLA alleles, contributes to disease risk, not all genetically predisposed individuals develop Type 1 diabetes. Screening first degree relatives (FDRs) for islet autoantibodies (GAD65, IAA, IA-2, ZnT8) helps detect autoimmune activity. However, these serum markers arise only after T-helper cell activation, limiting early intervention opportunities. Since protein antigen recognition by B cells requires T-helper cell assistance through linked recognition, T cell activation precedes B cell activation and autoantibody production. Activation of these T cells leads to shedding of the immune-regulatory (activation) surface protein LAG-3 (Lymphocyte Activation Gene-3 or CD223), generating its soluble form, sLAG-3, that is detectable in circulation. We hypothesized that sLAG-3 may serve as an early biomarker of autoimmune activity preceding islet autoantibody development in type 1 diabetes.

Methods: Plasma sLAG-3 levels were measured longitudinally in female diabetes-prone NOD mice and analyzed in relation to islet antigen-specific $CD4^+$ T cell expansion and diabetes onset. To mechanistically link autoreactive T cell activation to sLAG-3 release. Naive autoreactive C6.6.9 TCR-transgenic (TCR-Tg) $CD4^+$ T cells were adoptively transferred into NOD.SCID mice and longitudinal assessment for plasma sLAG-3, beta-cell antigen specific $CD4^+$ T cell tetramer profiles, and circulating insulin (*Ins2*) mRNA to determine ongoing beta-cell stress. In parallel, sLAG-3 levels were analyzed from different human cohorts, including FDRs of individuals with type 1 diabetes, using cross-sectional and longitudinal approaches.

Results: In murine models, elevated sLAG-3 correlated with expansion of islet-specific $CD4^+$ T cells that preceded hyperglycemia and diabetes onset. In the adoptive transfer model, early increases in sLAG-3 and circulating *Ins2* mRNA marked immune activation and emerging beta-cell stress prior to overt diabetes. In our human cohorts, sLAG-3 was detectable in autoantibody-negative and single-autoantibody-positive FDRs, with higher

levels observed in progressors compared to non-progressors, and associated with high-risk HLA genotypes.

Conclusions/interpretation: These findings identify sLAG-3 as a candidate biomarker of early T cell activation in type 1 diabetes that may precede islet autoantibody development. Integration of sLAG-3 with antigen-specific T cell and beta-cell stress markers could improve early risk stratification and inform preventive strategies before substantial loss of beta-cell. Prospective longitudinal studies aligned to seroconversion are required to validate sLAG-3 as a surrogate marker of early disease activity.

Keywords: Type 1 diabetes, sLAG-3, T cell activation, autoimmunity, beta-cell destruction, biomarker, islet autoantibodies, *Insulin* mRNA, immune infiltration.

Abbreviations

ChgA	Chromogranin A
FACS	Fluorescence-Activated Cell Sorting buffer
FDR	first degree relative
GAD65	Glutamic Acid Decarboxylase 65 (isoform of GAD)
HLA	Human Leukocyte Antigen
IA-2	Islet Antigen-2 (a pancreatic β-cell antigen)
IAA	Insulin Autoantibody
IAPP	Islet Amyloid Polypeptide (also called amylin)
IFN-γ	Interferon-gamma
mRNA	messenger Ribonucleic Acid
NOD	Non-Obese Diabetic (mouse strain)
NOD.SCID	NOD. Severe combined immunodeficient
RPM	Revolutions Per Minute (common lab term, e.g., centrifugation speed)
TCR	T Cell Receptor
ZnT8	Zinc Transporter 8

Research in context

What is already known about this subject?

- Before the clinical onset of hyperglycemia, type 1 diabetes is characterized by a prolonged preclinical phase in which autoreactive B and T cells mediate progressive beta-cell destruction.
- Current risk stratification strategies rely mainly on genetic susceptibility (genomic DNA) and the detection of islet autoantibodies in plasma/serum.
- Islet autoantibodies arise only after $CD4^+$ T cell activation and therefore do not capture the earliest stages of immune dysregulation.
- Consequently, biomarkers that directly reflect early pathogenic T cell activity prior to, or independent of, seroconversion remain limited and insufficiently validated.

What is the key question?

Can plasma sLAG-3 levels, beta-cell antigen-specific $CD4^+$ T cell tetramer expression, and circulating *Ins2* mRNA serve as very early biomarkers of autoimmune activity in type 1 diabetes and serve to better inform risk stratification, thereby informing preventive intervention strategies for the clinician?

What are the new findings?

- sLAG-3 increases transiently during early antigen-specific $CD4^+$ T cell activation stage, precedes hyperglycemia in mouse models, and is elevated in autoantibody-negative and single-autoantibody-positive first-degree relatives who later progress to type 1 diabetes.
- sLAG-3 was associated with beta-cell antigen-specific $CD4^+$ T cell expansion, assessment of stress induced beta cell *Ins2* mRNA release and high-risk HLA genotypes, indicating early autoimmune activation rather than established disease.

How might this impact clinical practice in the foreseeable future?

These findings support sLAG-3 as a candidate early biomarker of T cell activation, before or at the earliest stages of islet autoantibody development in some at-risk individuals. Integration of plasma sLAG-3 with beta-cell antigen specific $CD4^+$ T cell profiling and

119 insulin mRNA measurements could complement current autoantibody-based screening,
120 improve risk stratification, and enable earlier preventive interventions to preserve beta-
121 cell function in patients at-risk for type 1 diabetes.

122

Introduction

Type 1 diabetes is a complex, heterogeneous, and polygenic autoimmune disease characterized by $CD4^+$, $CD8^+$-T cell and B cell mediated destruction of pancreatic beta-cells, resulting in insulin deficiency and hyperglycemia [1-3]. Despite extensive research, the mechanisms driving this aberrant immune positive beta-cell interaction remain incompletely understood [4]. Type 1 diabetes affects 9.5 million people globally (2 million in USA). The global incidence is rising globally by 2-3% annually, outpacing the prevalence of high-risk HLA and other genetic alleles, indicating that environmental factors, including viral infections and oxidative stress, likely contribute to disease development [5-7]. First-degree relatives of type 1 diabetes patients, particularly those carrying HLA-DR3/-DQ2 and/or -DR4/-DQ8 HLA haplotypes, are at elevated genetic risk for type 1 diabetes. Patients and at-risk individual can be screened for islet autoantibodies in plasma/serum and HLA typing genomic DNA. Current biomarkers such as GAD65, insulin, IA-2 and ZnT8 autoantibodies are typically become detectable only after substantial beta-cell loss, indicating a clinically silent window of early immune dysregulation that remains undetected [8, 9]. Thus, there is a crucial and yet unmet need to validate this silent window for biomarkers capable of identifying type 1 diabetes at the earliest pre-seroconversion stages of autoimmunity.

The FDA approval of teplizumab, an anti-CD3 lymphodepleting immunomodulatory therapy, represents a major advance in our field that, demonstraties that disease onset can be delayed when treatment is initiated post-autoantibody seroconversion [10]. Nevertheless, full disease prevention remains challenging, as intervention at this stage occurs after significant beta-cell injury [11]. Since seroconversion occurs only after immune tolerance is breached and self-reactive $CD4^+$ T cells are activated, earlier biomarkers that detect pathogenic immune activity and distinguish progressors from non-progressors are urgently needed to inform prevention strategies [11-13]. Autoantibodies primarily reflect loss of immune tolerance but arise only after $CD4^+$ T cells provide help for B cell activation and antibody production [10, 11]. Early antigen-specific $CD4^+$ T cells deliver essential co-stimulatory signals and cytokines that drive B cell proliferation, isotype class switching, and differentiation into plasma cells that produce high-affinity

153 autoantibodies against beta-cell antigens [14]. While both genetic and environmental
154 factors likely contribute to $CD4^+$ T cell activation, the initiating triggers remain unclear [15,
155 16].

156 During T cell activation, a cellular metalloprotease (ADAMs-17) enzymatically cleaves the
157 lymphocyte activation gene-3 protein from the cell surface, releasing sLAG-3 into
158 circulation as a T cell activation marker [12, 14, 15]. LAG-3 is a co-inhibitory receptor
159 expressed on regulatory T cells that is structurally similar to CD4 [17]. Increase sLAG-3
160 levels, previously associated with strong immune responses in cancer, and Graves'
161 Disease, appears to predict emerging autoimmunity in type 1 diabetes prior to
162 autoantibody detection [16, 18, 19]. Concurrently, in beta cells proinflammatory stress
163 mediate release of *insulin* mRNA into circulation, representing another promising early
164 marker of beta-cell dysfunction [20-22]. However, the lack of early biomarkers that can
165 be used to identify at-risk individuals before seroconversion, highlights the need for
166 enhanced assays capable of detecting both sLAG-3 and *insulin* mRNA to monitor early
167 immune activity and beta-cell health.

168 To evaluate the feasibility of these proposed biomarkers panel, we conducted a
169 preliminary study integrating plasma sLAG-3 quantification via monoclonal antibody-
170 based ELISA assay with beta-cell antigen-specific $CD4^+$ T cell tetramer profiling. This
171 combinatorial assay was applied to longitudinal plasma samples from female diabetic-
172 prone NOD mice, a human cohort from the Diabetes Evaluation in Washington (DEW)
173 study, and cross-sectional autoantibody-positive samples from the Stanford Diabetes
174 Biobank. In these preclinical and clinical samples, we observed early increases in plasma
175 sLAG-3 coincided with rising frequencies of beta-cell antigen-specific $CD4^+$ T cells. Our
176 results accurately predicting impending diabetes onset and supporting the potential utility
177 of this biomarker combination. We further examined early immune activation using a
178 longitudinal adoptive-transfer model of autoimmune diabetes in which naïve islet-reactive
179 $CD4^+$ T cells from NOD.C6.6.9 TCR-transgenic mice were transferred into
180 immunodeficient NOD.SCID recipients. This reductionist system enables real-time
181 monitoring of autoreactive T cell antigen engagement, activation, expansion, antigen
182 engagement, and effector differentiation. We assessed plasma sLAG-3 concentration,

183 CD4$^+$ T cell tetramer positivity, and circulating *insulin* mRNA levels as biomarkers of beta-
184 cell health and disease progression [20]. Notably, the early rise in circulating *Ins2* mRNA
185 in whole blood sapless preceded hyperglycemia and coincide with increases in immune
186 cell infiltration into the pancreatic islets, suggesting that immune-driven β-cell dysfunction
187 disrupts insulin protein synthesis and secretion far earlier than previously recognized [23-
188 25]. These findings support the use of metabolic markers to detect early beta cell
189 vulnerability, that could complement immune-activation biomarkers of immune activation
190 and uncover targets to preserve insulin secretion. Additionally, human studies further
191 confirm an increase in sLAG-3 in plasma of single autoantibody-positive first-degree
192 relatives of individuals with type 1 diabetes compared to individuals who are
193 autoantibody-negativity, reinforcing its potential as an early biomarker. Combined
194 monitoring of sLAG-3 and CD4$^+$ T cell tetramer expression, along with circulating *Ins2*
195 mRNA, may enable earlier type 1 diabetes detection and inform type 1 diabetes
196 intervention trial before substantial beta-cell loss and clinical onset [20, 24].

197 **Methods**

198 **Animal Models and Diabetes Assessment**

199 NOD/ShiLtJ (Strain 001976), NOD.Cg-Prkdc$^{scid/J}$ (Strain 001303), and C57BL/6 (Strain
200 000664) male and female mice were obtained from Jackson Laboratory. Beginning at 4
201 weeks of age, NOD/ShiLtJ mice were routinely monitored for glucosuria in 3-day intervals
202 during adoptive transfer studies. Blood glucose was measured in mice positive for
203 glucosuria, and overt diabetes was defined as two to three consecutive readings >300
204 mg/dL. Blood glucose was measured by puncturing the last 1 mm of the tail and
205 dispensing one drop of blood on a Contour next® disposable test strip and glucometer.
206 All mice were bred and maintained under specific pathogen-free conditions at Indiana
207 University's BRTC, managed by LARC. Animal experiments were conducted in
208 accordance with Animal Research: Reporting of In Vivo Experiments (ARRIVE) guidelines
209 under protocols approved by the Indiana University (IU) School of Medicine Animal Use
210 Committee.

211 **Research participant's samples**

212 Plasma from healthy controls, type 1 diabetes participants, and FDRs were provided by
213 Children's Hospital of Pittsburgh, Stanford University School of Medicine (IRB Protocol
214 #35453), University of Florida, and University of Queensland. Samples were stored at
215 −80°C until analyzed. Participants with type 1 diabetes ranged in age at onset (1 to 16
216 yrs old) and duration of disease (1 to 6 years post-onset). FDRs were tested for auto-
217 antibodies to GAD65, IAA, and IA2 by standard radioimmunoassay. Plasma samples
218 were collected from two cohorts of healthy controls, younger participants aged 25-35 and
219 older participants aged 55-65 years old who were recruited into the Sound Life Project for
220 measuring the sLAG-3 level from research participant before and after covid vaccination.
221 Samples were collected with approval from Benaroya Research Institute, Seattle, WA
222 review board (IRB19-045) and the Stanford University School of Medicine institutional
223 review board (IRB 35453). All participants provided written informed consent. Prospective
224 cohort longitudinal studies for measuring the sLAG-3 from Diabetes Evaluation in
225 Washington Study (DEWIT) enrolled infants from the general population (n=39) carrying
226 increased-risk HLA-DR-DQ genotypes identified by newborn screening, as well as first-
227 degree relatives of individuals (n=13) with or without type 1 diabetes regerdless of HLA
228 genotype. All participants underwent HLA screening, though eligibility criteria varied
229 across sites. Follow-up began between 2 months and 21.6 years of age and continued at
230 3 to 36 month intervals for up to 26 years, with type 1 diabetes diagnosed according to
231 American Diabetes Association criteria. All protocols were approved by local institutional
232 review boards, and de-identified data were submitted to IBM Research. The harmonized
233 cohort comprised median 10 visits, 8.7 years follow-up; 17% reported a family history of
234 type 1 diabetes. For key analyses, it was examined the infant-toddler subcohort, restricted
235 to subjects tested for insulin, IA-2, and GAD autoantibodies by age 2.5 years. The infant-
236 toddler cohort included median 12 visits, 10.4 years follow-up [26].

237 **Estimating soluble LAG-3 levels from NOD and human plasma**

238 NOD/ShiLtJ and NOD.Cg-Prkdc$^{scid/J}$ mice from different experimental groups were retro-
239 orbitally bled for plasma every other week from 4 to 16 weeks of age. Plasma was isolated

240 by centrifugation at 3000 × RPM for 10 minutes at 4°C. Mouse sLAG-3 was measured by
241 sandwich ELISA using 96-well high-affinity plates (Corning #3361) coated overnight at
242 4°C with 5 μg/mL monoclonal anti-LAG-3 (C9B7W, InVivoMab #BE0174). LAG-3
243 standard was purchased from R&D (Catalog: AF3328) antibody pairs for mouse
244 compatible were purchased from Jackson Immuno Research, performed according to
245 manufacturer's protocol. Human plasma from three institutions was analyzed using
246 Human LAG-3 DuoSet ELISA (R&D #DY2319B). All samples were run in triplicate, read
247 at OD450 nm on a SpectraMax-iD5, and analyzed with SoftMax-Pro 7.0.2.

248

249 **Plasma sLAG-3 evaluation from DEWIT cohort study and Stanford Biobank**

250 Human plasma samples were analyzed for sLAG-3 levels by the MSD U-PLEX platform
251 using sandwich immunoassays for protein targets and a competitive assay for neopterin,
252 with electrochemiluminescence detection. MULTI-ARRAY® 96-well plates contained
253 sLAG-3 capture antibodies, Sulfo-Tag detection antibodies, calibration standards, and
254 diluents. The Indiana University Translational Core processed 50 μL of each sample in
255 triplicate. Mean concentrations were reported, with values below the limit of detection
256 (LOD) assigned the LOD. Plate-specific control coefficients of variation (CVs) were
257 calculated for sLAG-3.

258 **Estimating sLAG-3 from covid vacationed research participants**

259 sLAG-3 level from covid vacationed research participants plasma was measured using
260 the Olink proximity extension assay on the Olink Explore 1536 platform's oncology panel
261 [27]. Samples were randomized across plates to balance age and sex, with longitudinal
262 samples from the same participant run on the same plate. Bridging controls were included
263 in each batch for cross-batch normalization. Protein expression values were first
264 normalized within wells using internal extension controls (IgG antibodies with matched
265 oligos), then standardized across plates using triplicate inter-plate pooled serum controls.
266 Data were subsequently intensified across all samples, and final normalized relative
267 protein quantities were reported as NPX values.

268 **In vivo viral infection incidence study**

269 Eight-week-old C57BL/6 mice were intraperitoneally infected with 100 PFU
270 Coxsackievirus B (CVB3 #ATCC® VR-30™) in HBSS under specific pathogen-free
271 conditions. Blood was collected via retro-orbital bleeding at baseline and on days 3, 6, 9,
272 12, 16, and 21 post-infections. Plasma was isolated by centrifugation and stored at -80°C.
273 sLAG-3 levels were quantified using standard ELISA, while intracellular IFN-γ in $CD4^+$
274 and $CD8^+$ T cells was measured by flow cytometry to assess immune activation during
275 infection.

276 **Adoptive transfer**

277 Spleens from 8-week-old female NOD congenic C6.6.9 TCR-Tg mice were harvested
278 sterilely, mechanically homogenized, passed through a 40 μm strainer, washed, and
279 resuspended in cold DMEM with 10% FBS. Lymphocytes were isolated via Ficoll-Paque
280 density gradient, washed twice with PBS, and 5×10^6 cells were retro-orbitally transferred
281 into 8-week-old female NOD.Cg-$Prkdc^{scid/J}$ recipients. Post-transfer, mice were monitored
282 for diabetes progression by blood glucose and bled every three days to measure plasma
283 sLAG-3, activation markers and co-inhibitory receptor (CD69, CD44, LAG-3), and $CD4^+$
284 T cell reactivity to beta-cell antigens (ChgA, InsB9-23, IAPP) using tetramers. Mice with
285 >300 mg/dL glucose on two readings were euthanized for spleen and pancreas for further
286 analyses.

287 **Staining and flow cytometry analysis**

288 To assess T cell mediated immune activation in autoimmune and viral contexts,
289 lymphocytes were analyzed by flow cytometry. NOD/ShiLtJ mice were longitudinally bled
290 during diabetes progression, and NOD.SCID mice were sampled after adoptive transfer.
291 For viral studies, $CD4^+$IFN-γ^+ and $CD8^+$IFN-γ^+ T cells were analyzed from C57BL/6 blood.
292 Lymphocytes were isolated, RBCs lysed, and cells resuspended in FACS buffer. Cells
293 were stained with eFluor-780 viability dye and surface markers including CD45-FITC,
294 CD4-PerCP-Cy5.5, CD8-APC, CD69-PE/Cy7, CD25-PE, LAG-3-BV650, CD71-APC,
295 CD98-PE/Cy7, and Glut-1-PE. For beta-cell antigen specific, APC-ChgA, BV421- InsB9-

296 23, and PE-IAPP tetramers were used. Intracellular IFN-γ-PE staining was performed
297 using the Fixation & Permeabilization Buffer Kit protocol (eBiosciences FOXP3 Fix/Perm
298 kit, Cat #00-5523-00). Data were analyzed using FlowJo-v10.

299 **Cytokine measurement by ELISA**

300 Plasma from CVB-infected C57BL/6 mice was collected at multiple time points and
301 analyzed for IFN-γ by ELISA. High-affinity 96-well plates were coated overnight at 4°C
302 with 25 ng/mL monoclonal rat anti-murine IFN-γ in carbonate buffer (pH 9.6). Mouse IFN-
303 γ ELISAs were performed using BD antibody pairs following the manufacturer's protocol.
304 Mean OD450 values were recorded on a SpectraMax-iD5 microplatereader, analyzed
305 using SoftMax Pro-7.0.2.

306 **Histology and Immunofluorescence**

307 Pancreata from control, diabetic, and post-adoptive transfer NOD.SCID mice (days 12
308 and 15) adoptively transferred NOD.SCID mice were harvested at diabetes onset, fixed
309 in 4% paraformaldehyde for 4 hours at 4°C, washed with distilled water, and processed
310 for paraffin embedding, and stained with hematoxylin and eosin to assess tissue
311 architecture and immune infiltration following standard protocol. For
312 immunofluorescence, pancreata cryoprotect overnight at 20% sucrose in PBS. Tissues
313 were embedded in OCT, frozen, and stored at -80°C. Cryosections (6 μm) were prepared
314 using a cryostat. Sections were blocked with 5% normal donkey serum and 1% BSA,
315 incubated overnight at 4°C with monoclonal CD3, insulin, F4/80, and B220 primary
316 antibody, followed by fluorophore-conjugated secondary antibodies. Similarly, APC-
317 ChgA, BV421- InsB9-23, and PE-IAPP tetramers antibody are also used. Nuclei were
318 counterstained with DAPI. Images were acquired on a Zeiss LSM-800 and analyzed using
319 ImageJ.

320 **RNA isolation and ddPCR**

321 Total RNA was isolated from the blood of adoptively transferred NOD.ScidSCID mice
322 using RNAprotect Animal Blood Tubes (cat. #76544) and the RNeasy Protect Animal

323 Blood Kit (cat. #73224) per manufacturer instructions. RNA concentration was measured
324 with a NanoDrop-2000 (Thermo Fisher Scientific). cDNA was synthesized using M-MLV
325 Reverse Transcriptase (Invitrogen) according to the manufacturer's protocol. Droplet
326 digital PCR (ddPCR) was performed to quantify *Ins2* mRNA. Briefly, 2 µL of cDNA was
327 combined with 10 µL ddPCR Supermix for Probes (1863024) and 1 µL TaqMan primer
328 (Cat #4427975) that target *Ins2* transcript and the volume was adjusted to 20 µL with
329 RNase/DNase-free water. Synthetic *Ins2* cDNA was used as a positive control and RNAse
330 free water was used negative controls. Droplets were generated with QX200 AutoDG,
331 PCR on a C1000 Thermal Cycler, and read with QX200 droplet reader. Data (copies/µL)
332 were analyzed using QuantaSoft software.

333 **Statistical Analysis**

334 Data analysis was performed using GraphPad Prism10. Pairwise comparisons were
335 performed using unpaired or paired two-tailed Student's t-tests. Interactions between two
336 groups with two variables (e.g., time or treatment, pre-post-vaccination) were determined
337 using a one-way ANOVA followed by an appropriate post hoc test. Sample sizes (n),
338 means, error bars, and statistical methods are described in figure legends. A p-value
339 <0.05 indicates statistical significance.

340 **Results**

341 **Plasma sLAG-3- levels track spontaneous diabetes onset in NOD mice**

342 LAG-3 (CD223) is a co-inhibitory receptor expressed by CD4+CD25+CD127lo regulatory
343 T (Treg) cells and other regulatory immune cell subsets [28, 29]. We previously proposed
344 that protein enzyme catalytic liberation of LAG-3 from the surface of CD4 Tregs
345 (solubilized or sLAG-3) is a key biomarker, indicative of loss of tolerance to pancreatic
346 islet beta cell antigens in autoimmune-prone NOD mice [30]. To determine whether
347 soluble LAG-3 In plasma/serum reflects early autoimmune activation, we followed female
348 NOD mice longitudinally from 4-16 weeks of age, measuring plasma sLAG-3 and blood
349 glucose biweekly (Fig.1a). Plasma sLAG-3 was low at 4 weeks of age, increased
350 significantly during 6 to12 weeks, reflecting early T cell activation and then declined to

351 near-baseline levels by 16 weeks of age (Fig. 1b). This window of elevated sLAG-3
352 coincided with the prediabetic period when insulitis is known to expand in NOD mice [31].
353 In contrast, blood glucose remained normal through 12 weeks and began to rise around
354 16 weeks of age as overt, clinical diabetes appeared (Fig. 1c). Importantly, a significant
355 positive correlation was observed between peak sLAG-3 levels and the timing of diabetes
356 onset in the female NOD cohort (Fig. 1d), indicating that higher early sLAG-3 levels are
357 associated with greater likelihood of progression to hyperglycemia in this model.

358 **Beta cell antigen-specific CD4$^+$ T cells expand in parallel with sLAG-3 during**
359 **spontaneous disease**

360 We next examined whether beta-cell antigen specific CD4$^+$ T cells show similar temporal
361 dynamics during spontaneous disease in female NOD mice from the same longitudinal
362 cohort (Fig. 1a). Using MHC class II tetramers for the pancreatic islet beta cell antigens
363 InsB923, ChgA, and IAPP, we observed- a significant increase in both the frequency and
364 absolute number of tetramer positive CD4$^+$ T cells between 6 and 12 weeks of age (Fig.
365 2a, b). Mean fluorescence intensity (MFI) of tetramer staining also increased over this
366 interval (Fig. 2c), consistent with either higher TCR occupancy or enrichment of
367 higher-affinity clones. Among the three specificities, InsB9-23$^+$ CD4$^+$ T cells were the
368 most abundant at 6 weeks and increased further by 12 weeks of age. In contrast, ChgA
369 and IAPP-specific cells started at a lower frequency and expanded later time points,
370 suggesting a progressive broadening of beta cell antigen recognition within the CD4$^+$
371 compartment. However, consistent with Fife et al. findings, reveal that in spontaneous
372 diabetes, multiple autoreactive T cell populations infiltrate the islets, including ChgA-
373 specific BDC2.5, and IAPP-reactive BCD6.9 T cells. Among these, BDC2.5 T cells are
374 the most pathogenic, likely owing to the robust production of IFN-g and TNF-a [32] ,
375 whereas insulin-reactive T cells, despite their abundance, exhibit limited immuno-
376 pathogenicity [33]. The rise in tetramer-positive cells coincided with the period of elevated
377 plasma sLAG-3 and preceded the clinical onset of hyperglycemia (Fig. 1b, c, and 2d).
378 Linear regression analysis confirmed a significant positive association between plasma
379 sLAG-3 levels and the frequency of beta-cell antigen–specific CD4$^+$ T cells in our NOD
380 murine studies (Fig. 2e), linking systemic sLAG-3 shedding to antigen-specific T cell

activation and loss of tolerance to beta cells and their protein antigen during early autoimmune progression.

Adoptive transfer of C6.6.9 CD4$^+$ T cells reveals early sLAG-3 induction and beta-cell stress

To further study the relationship between beta-cell injury, beta-cell antigen–specific CD4$^+$ T cells activation/expansion and release of sLAG-3 release and beta-cell injury, we adoptively transferred splenocytes from NOD.C6.6.9 TCR transgenic mice into NOD.SCID recipients (Fig. 3a). Donor mice express the BDC-6.9 TCR but lack the cognate IAPP-derived hybrid peptide, so their CD4$^+$ T cells remain naïve prior to transfer. After adoptive transfer, recipient NOD.SCID mice undergo a prediabetic phase followed by a rapid metabolic -shift with in, blood glucose began to rise by approximately 7 weeks after transfer and exceeded 400 mg/dL by week 10 (Fig. 3b, c and ESM Fig. 2b). Plasma sLAG-3 levels increased early following adoptive transfer, peaking between days 12-15 after adoptive transfer and then declining as diabetes developed (Fig. 3d; ESM Fig. 2a). In line with the data from sLAG-3 secretion, circulating levels of *Ins2* mRNA showed a similar early increase (Fig. 3e), indicating ongoing beta-cell stress during the same interval. *Ins2* mRNA displayed a modest positive association with sLAG-3 (Fig. 3f), but neither marker correlated positively with blood glucose, consistent with the idea that substantial immune and beta-cell stress precede overt hyperglycemia (Fig. 3g). However, sLAG-3 showed an inverse correlation with blood glucose when later time points were included (Fig. 3h), indicating high sLAG-3 in circulation early during autoreactive T cell activation followed by a decline as beta-cell mass is lost. Flow cytometry revealed dynamic redistribution of donor C6.6.9 CD4$^+$ T cells- over time, with expansion in the periphery followed by accumulation in the pancreas and secondary lymphoid organs (Fig. 3i). Histopathological analysis of pancreata from diabetic recipients showed marked signs of immune cell infiltration and insulitis, with extensive islet destruction (Fig. 3j). Together, these data confirm that beta cells antigen specific CD4$^+$ T cells are sufficient to drive diabetes in this model and that early activation is accompanied by a transient rise in plasma sLAG-3 and beta-cell *Ins2* mRNA.

410 **Longitudinal assessment of antigen specific CD4$^+$ T cell activation and beta-cell**
411 **antigen tetramer profiles in adoptively transferred mice.**

412 We next characterized the activation state and antigen specificity of CD4$^+$ T cells in
413 peripheral blood of adoptively transferred NOD.SCID mice every three days. Shortly after
414 transfer, CD4$^+$ T cells exhibited a pronounced activation surge defined by increased
415 CD25$^+$ and CD69$^+$ frequencies, peaking between days 3-9 following adoptive transfer
416 (Fig. 4a; ESM Fig. 3a). Concomitantly, the frequency of ChgA$^+$, InsB9-23$^+$, and IAPP$^+$
417 tetramer-positive CD4$^+$ T cells transiently rose between 9 and 15-days post-transfer and
418 then declined as cells redistributed into tissues (Fig. 4b; ESM Fig. 3b). LAG-3 expression
419 on CD4$^+$ T cells also increased early and then decreased among adoptively transferred
420 CD4 T cells, consistent with the pattern of soluble LAG-3 detected in plasma. Therefore,
421 to address the mechanism underlying the emergence of these newly detected antigen-
422 specific T cell populations, we performed immunofluorescence staining of pancreata at
423 days 12 and 15 post adoptive transfer. We found that tetramer-positive cells,
424 particularly -ChgA$^+$, were more abundant at day 12 than day 15 (Fig. 4c, d), mirroring the
425 transient early peak observed in blood. At diabetes onset, analysis pancreatic tissue
426 revealed that CD69 expression was significantly increased on pancreatic CD4$^+$ T cells
427 compared with blood. In contrast, CD25 expression was relatively higher in circulating
428 CD4+ T cells (Fig. 4e; ESM Fig. 3c). Tetramer positive CD4$^+$ T cells specific for ChgA,
429 InsB9-23, and IAPP were most enriched in the pancreas compared with spleen and blood
430 (Fig. 4f; ESM Fig. 3d), indicating preferential homing and/or retention of autoreactive
431 CD4$^+$ T cells at the site of beta-cell destruction. Consistent with findings by Bettini and
432 Vignali et al., T cells that are not specific for islet beta-cell antigens do not persist within
433 the pancreatic islets and exit once cognate antigen recognition fails to occur [34].

434 **Beta-cell antigen driven metabolic reprogramming and immune infiltration in the**
435 **pancreas**

436 To assess metabolic changes accompanying antigen driven T cell activation, we examine
437 the immune infiltration in pancreas and quantified nutrient transporter expression on CD4$^+$
438 T cells isolated from blood, spleen, and pancreas at diabetes onset in adoptively

transferred NOD.SCID mice (Fig. 5a). Immunofluorescence confirmed dense infiltrates of $CD3^+$ T cells along with $B220^+$ B cells and $F4/80^+$ macrophages in diabetic pancreata compared with controls, together with loss of insulin positive beta-cells (Fig. 5b), suggests that autoreactive T cells maybe directly and indirectly by activating macrophage the local milieu to support B cell help and drive metabolic programs sustaining effector function [35-37]. Flowcytometry profiling demonstrated that $CD4^+$ T cells from pancreatic tissue expressed higher frequencies of Glut-1^+ and $CD98^+$ cells than those from spleen or blood (Fig. 5c; ESM Fig. 5a, b), consistent with increased glucose and amino acid uptake in tissue-resident effector cells indicating cell activation, proliferation, and anabolic metabolism, while decreased expression suggests a resting or differentiated state. CD98 expression was high across compartments at diabetes onset, whereas $CD71^+$ $CD4^+$ T cells were more frequent and showed higher MFI in the spleen than in blood or pancreas (Fig. 5d; ESM Fig. 5a, b), suggesting ongoing proliferative expansion in secondary lymphoid organs. These data indicate that antigen encounter in this model is associated with both immune infiltration of the pancreas and tissue-specific metabolic activation of $CD4^+$ T cells. Targeting these metabolic checkpoints may offer a strategy to selectively dampen pathogenic T-cell responses in early T1D [38-40].

Broadening and epitope diversification of IAPP-specific $CD4^+$ T cells Co-recognizing ChgA and InsB9-23 antigen.

To explore how antigen recognition evolves during disease, we re-analyzed adoptive transfer flow-cytometry data by gating on $CD4^+IAPP^+$ T cells and then assessing additional binding to ChgA and InsB9-23 tetramers over time (Fig. 6a; ESM Fig. 6a, b), This approach highlights the underutilized potential of BCR and TCR repertoire dynamics in diagnostic medicine. At baseline, very few $CD4^+IAPP^+$ cells co-stained with ChgA or InsB9-23 tetramers (Fig. 6b). After transfer into NOD.SCID recipients, the proportion and absolute number of $CD4^+IAPP^+ChgA^+$ and $CD4^+IAPP^+InsB9\text{-}23^+$ T cells in blood increased progressively and reached maximal levels around day 12 post-adoptive transfer (Fig. 6c, d). At diabetes onset, both dual positive subsets were enriched in pancreatic tissue compared with spleen (Fig. 6e, f). These findings indicate that within the IAPP-defined autoreactive pool, there is a broadening of tetramer-defined antigen

469 recognition over time, with preferential accumulation of multi-positive cells in the pancreas
470 during overt disease.

471 **sLAG-3 patterns in human T1D, FDRs, and longitudinal DEWIT cohorts**

472 We then examined whether the sLAG-3 patterns observed in mice were recapitulated in
473 human cohorts. In a cross-sectional analysis of individuals with type 1 diabetes up to six
474 years after diagnosis and age-matched healthy controls, serum sLAG-3 levels did not
475 differ significantly between groups (Fig. 7b). This suggests, as seen in the mouse
476 experiments, that by the time of established disease, the early activation signal captured
477 by sLAG-3 is not readily detectable. In contrast, when first-degree relatives were stratified
478 by autoantibody status, autoantibody negative and single autoantibody FDRs displayed
479 significantly higher sLAG-3 levels than multi-autoantibody FDRs, T1D subjects, and non-
480 FDR- controls, indicating early T-cell activation (Fig. 7c). Consistent with this, sLAG-3
481 levels showed no significant differences among T1D patients regardless of autoantibody
482 status (ESM Figure 7a), reinforcing that sLAG-3 is not a marker of late-stage disease
483 burden.

484 Longitudinal analysis of the DEWIT cohort using MSD-based high sensitive assays,
485 chosen for their suitability in repeated-measure analyses, showed that sLAG-3 levels
486 were generally higher in females than males across both FDR and general population
487 participants. (Fig. 7e, f). When participants were stratified by outcome, progressors
488 exhibited a gradual rise in sLAG3 over time, culminating in a distinct peak just before
489 diabetes diagnosis and a subsequent decline after onset. In contrast non-progressors
490 showed no consistent change (Fig. 7g, j; ESM Fig. 7b). The sLAG-3 levels also tend- to
491 decrease with increasing disease duration among individuals with type 1 dibetes (ESM
492 Fig. 7c). In FDRs, sLAG-3 concentrations were highest in autoantibody negative and
493 single-autoantibody positive individuals and progressively lower in those with multiple
494 autoantibodies, with the single 4-autoantibody-positive individual showing the lowest
495 value (Fig. 7h). This inverse relationship between sLAG-3 and autoantibody burden was
496 not observed in general-population subjects (Fig. 7i), suggesting that early sLAG-3
497 elevation is most apparent in genetic or familial at-risk individuals. Additionally, non-

498 diabetic individuals showed higher sLAG-3 concentrations compared with diabetic
499 subjects among GADA positive, IA2A positive and ZnT8A positive participants in first-
500 degree relatives, but no significant difference observed in general population. In contrast,
501 IAA-positive groups showed no significant differences in sLAG-3 between diabetic and
502 non-diabetic individuals, indicating that alterations in circulating sLAG-3 are associated
503 with diabetes status in specific autoantibody-defined subgroups (ESM Fig. 7d-g). Finally,
504 sLAG-3 levels were higher in subjects carrying high risk HLA alleles such as DRB1**04*
505 (DR4) *and DQA1**03:01-DQB1*03:02 (DQ8) compared with those lacking these risk
506 genotypes (Fig. 7k). This result support a linking between genetic susceptibility and the
507 magnitude of early immune activation.

508 **sLAG-3 dynamics during COVID-19 vaccination and CVB infection**

509 To test whether sLAG-3 reliably marks early T cell activation in nonautoimmune contexts,
510 we measured sLAG-3 following COVID-19 vaccination in healthy adults and during
511 Coxsackievirus B3 (CVB3) infection in mice. In vaccinated adults, plasma sLAG-3
512 (measured by Olink as NPX values) increased significantly by 10 days after vaccination
513 compared with pre-vaccination levels, with most donors showing a clear upward shift (Fig.
514 8a, b). This transient increase occurred in the expected window for vaccine induced T cell
515 responses and before the mature humoral response.

516 In CVB infected C57BL/6 mice, plasma sLAG-3 was minimal at baseline, start to increase
517 by day 3, and peaked between days 6-9 before declining toward baseline by day 30 (Fig.
518 8c, d). Plasma IFN-γ levels followed a similar pattern with a marked increase around day
519 6 (Fig. 8e). Flow cytometry revealed a concurrent expansion of IFNγ-producing $CD4^+$ and
520 $CD8^+$ T cells and increased expression of activation markers CD25 and CD69 in
521 peripheral blood (Fig. 8f-i; ESM Fig. 8). These data confirm that sLAG-3 is a sensitive and
522 dynamic marker of early T-cell activation in both vaccine and viral infection settings.

523 **Discussion**

524 Our goal was to determine whether soluble LAG-3 is useful serve as a biomarker of early
525 T cell activation relevant to type 1 diabetes pathogenesis. Across spontaneous and

526 adoptive transfer NOD mouse models, human FDR and longitudinal type 1 diabetes
527 cohorts, and independent vaccine and viral infection systems. We consistently found that
528 sLAG-3 concentrations in plasma/serum rises significantly early during T cell activation
529 and declines as responses contract or as overt autoimmune diabetes develops. These
530 observations support sLAG-3 as a candidate biomarker of early T cell activation and
531 warrant further evaluation of its utility for staging autoimmune risk [16].

532 In NOD mice, plasma sLAG-3 increased between 6-12 weeks of age and returned to near
533 baseline by 16 weeks, while blood glucose remained normal until around 16 weeks of
534 age, when overt diabetes onset occurred. Consistent with our findings, Mathews and
535 Ludlow, demonstrated that subtle blood glucose dysregulation precedes overt diabetes
536 and extend extends this work by providing an immunological basis for these early
537 changes [41]. Their results suggest that early blood glucose elevations reflect increased
538 antigen-specific, immune-mediated beta-cell stress driven in part by BDC-2.5 reactive
539 $CD4^+$ T cells rather than global beta-cell loss, positioning early blood glucose
540 perturbations as a functional marker of immune activation preceding clinical diabetes [41].
541 Interestingly, we found that, beta-cell antigen specific $CD4^+$ T cells defined by InsB923,
542 ChgA, and IAPP tetramers expanded over the same 6-12-week window in the same
543 animal cohort. These findings correlated positively with sLAG-3 plasma concentrations.
544 Furthermore, in the C6.6.9 adoptive transfer model, sLAG-3 and *Ins2* mRNA rose rapidly
545 after adoptive transfer that peaked well before hyperglycemia. Histological and flow
546 cytometric evidence of insulitis and donor $CD4^+$ T cell accumulation in the pancreas.
547 Together, these results indicate that sLAG-3 is induced and persists during early antigen-
548 driven activation of autoreactive $CD4^+$ T cells and that its peak precedes frank metabolic
549 decompensation [42].

550 The adoptive transfer experiments also delineate how activation, tissue localization, and
551 metabolism among autoreactive $CD4^+$ T cells evolve during disease progression. CD25
552 and CD69 expression on peripheral $CD4^+$ T cells peaked early after transfer, paralleling
553 the sLAG-3 surge, and our detection of tetramer-positive cells. Subsequently, T cells
554 accumulated in the pancreas, where CD69 expression increases. $CD4^+$ T cells, that had
555 infiltrated the pancreas exhibit increased expression of Glut-1, CD98, and CD71

556 expression relative to blood and spleen, consistent with metabolic reprogramming of
557 effector cells in the inflamed target organ [43-49]. Within the IAPP specific pool, the
558 emergence and pancreatic localization of $CD4^+IAPP^+ChgA^+$ and $CD4^+$ $IAPP^+$ $InsB2\text{-}93^+$
559 subsets during diabetes indicated a progressive broadening of tetramer-defined antigen
560 recognition over time. Our results provide a coherent picture in which early antigen
561 encounter drives a transient systemic sLAG-3 signal, expansion and tissue homing of
562 antigen-specific $CD4^+$ T-cells and increased metabolic activity in the pancreas, long
563 before elevated blood glucose and failure of first phase insulin loss [33].

564 In humans, the cross sectional T1D vs non-diabetic control comparison showed no
565 difference in sLAG-3 levels up to six years post diagnosis, implying that the early
566 activation window identified in mice is not captured when sampling individuals with
567 established disease. In contrast, FDRs at earlier disease stages displayed a distinct
568 pattern: autoantibody negative and single autoantibody FDRs had higher sLAG-3 than
569 multi-autoantibody positive FDRs, T1D subjects, and non-FDR controls. Thus sLAG-3
570 declined with increasing autoantibody burden. Longitudinal data from the DEWIT cohort
571 further showed that progressors, but not non-progressors, exhibited a gradual rise in
572 sLAG-3 culminating in a peak immediately prior to diagnosis that declined thereafter.
573 sLAG-3 tended to be higher in individuals carrying higher risk type 1 diabetes HLA
574 genotypes. Taken together, these human data are consistent with a model in which sLAG-
575 3 in blood serving as a biomarker of autoimmunity during a relatively narrow early stage
576 of immune activation that precedes or is co-incident with a broadening of autoantibody
577 and auto-reactive T cell expansion prior to clinical onset in genetically susceptible
578 individuals [50, 51].

579 The current human dataset has important limitations that temper how strongly sLAG-3
580 can be positioned as a “surrogate marker before antibodies.” First, most of the human
581 analyses are cross-sectional. Even in the DEWIT cohort, the number of progressors with
582 dense longitudinal sampling is limited in. numbers. We therefore cannot yet systematically
583 align the timing of sLAG-3 concentration with individual seroconversion events to prove
584 that sLAG-3 consistently rises before the first islet autoantibody appears. Second, sLAG-
585 3 levels were measured using different assay platforms and in relatively small subgroups,

586 which constrains our ability to define robust thresholds or evaluate test characteristics
587 such as sensitivity, specificity, and predictive value. Third, the COVID-19 vaccine and
588 CVB infection experiments highlight that increases in sLAG-3 in blood occurs general
589 following T cell activation and may not be specific to autoimmunity. Eelevations in at-risk
590 individuals will likely need to be interpreted in the context of recent infections,
591 vaccinations, or other immune stimuli.

592 The COVID19 vaccination and CVB infection data nonetheless provide important context.
593 In both settings, sLAG-3 rose rapidly during the effector phase of the immune response,
594 coincided with increases in IFN-γ and T-cell activation but markers and returned to
595 baseline as the response resolved. These observations support the idea that sLAG-3 is
596 a sensitive and reversible readout of early T-cell activation. In type 1 diabetes, this
597 suggests that transient sLAG-3 elevations in FDRs are biologically plausible and that
598 serial measurements may be more informative than single time points, especially when
599 integrated with autoantibody profiles, islet or beta-cell antigen–specific T cell along with
600 detection of biorepositories, and plasma circulating insulin mRNA assessments in the
601 clinical context provide additional important data that may help distinguish autoimmunity
602 from other T cell-mediated immune responses.

603 Overall, our findings support as a cautious interpretation that sLAG-3 is a promising
604 biomarker of early T cell activation, detectable in some autoantibody-negative and single
605 autoantibody positive first-degree relatives and declining with increasing autoantibody
606 burden and after diabetes onset. When integrated with beta-cell antigen specific tetramer
607 profiling and markers of beta-cell stress such as circulating *Ins2* mRNA, sLAG-3 may help
608 define an early immunological phase characterized by autoreactive $CD4^+$ T cell activation
609 can be detected before substantial beta-cell loss is clinically evident. Larger, deeply
610 phenotype longitudinal cohorts will need to be tested to determine if assessment of sLAG-
611 3, autoantibody reactivity, markers of beta cell stress (circulating insulin mRNA in blood)
612 and T cell phenotypes comprise surrogate markers of type 1 diabetes risk or progression
613 and whether these markers are predictive of patients that go on to develop type 1 diabetes
614 clinically to determine how frequently it precedes seroconversion at the individual level.

Conclusion

In conclusion, our findings support sLAG-3 as a candidate early biomarker of T cell activation in type 1 diabetes, with evidence that sLAG-3 may be elevated before or at the earliest stages of islet autoimmunity in individual development in some at-risk individuals. We propose that tracking of beta-cell antigen specific $CD4^+$ T cell, circulating *Ins2* mRNA measurements, metabolic profiling, and analyses of B and T cell epitope spreading in conjunction with sLAG-3 reflects an early immunological state associated with autoreactive T-cell diversification rather than late-stage beta-cell loss. Nevertheless, larger longitudinal studies aligned to seroconversion are required to validate sLAG-3 as a surrogate marker of pre-autoantibody autoimmune disease and to define its utility for early risk stratification and therapeutic intervention.

Data and Resource Availability

The data sets generated and/or analyzed during the current study are available from the corresponding author on reasonable request.

Acknowledgements The authors thank Dr. Dario Vignali lab at University of Pittsburgh for providing the secondary antibody for the mouse sLAG-3 ELISA. We also thank to Dale Long - Facility Manager at NIH Tetramer Core Facility at Emory for providing tetramers and the Center for Diabetes and Metabolic Diseases for access to its instrumental facilities.

Funding This study was funded by the National Institute of Diabetes and Digestive and Kidney Diseases (NIDDK) under project 7R01DK132583, and Breakthrough Type 1 diabetes research Strategic Research Agreement (SRA) funds, under Project 1-PNF-2025-1642-A-N to Dr. Jon D. Piganelli, and R01DK129287 to Jason M. Spaeth. Farooq Syed was supported by a Breakthrough T1D (formerly JDRF) CDA (5-CDA-2022-1176-A-N and (CDA)/3-CDA-2025-1692-A-N) and Thomas Beatson Foundation (2024-010). This study is also supported by a NIH-R21 (1R21AI193399) award to Jon D. Piganelli and Farooq Syed.

Contribution statement J.D.P., S.R., F.S., and C.S. conceptualized the study. S.R. and J.D.P. designed all experiments; S.R. and M.L.P. performed experiments. S.R. analyzes all data and prepares all figures. F.S and J.R performed experiments on insulin mRNA, and M.E.S. conducted sLAG-3 assays in Covid-vaccinated participants. S. R and A.D.S. analyzed all confocal images. W.H help to collect the DEWIT cohort samples, A.T., E.S.H., E.M., and K.P.J. collect human plasma sample from Stanford Biobank, J.S. contributed to discussions and study design. S.R. and J.D.P. drafted the manuscript. S.F., M.L.P., J.S., A.D.S., K.P.J., J.S., and C.S. editing and finalizing it. All authors have no conflicts of interest.

652 **Figure Legends**

653 **Fig. 1** Plasma sLAG-3 correlates with disease incidence in NOD mice. (**a**) Experimental
654 design for longitudinally monitoring blood glucose and plasma sLAG-3 level from female
655 NOD mice. (**b**) Plasma sLAG-3 levels in NOD mice at different ages. (**c**) Longitudinal
656 monitoring of blood glucose levels. (**d**) Correlation between plasma sLAG-3 levels and
657 diabetes incidence in NOD mice. Data are presented as mean ± SEM (n=10-12 per
658 group). Statistical significance was determined using one-way ANOVA followed by
659 Bonferroni post-hoc testing; *$p<0.05$*.

660 **Fig. 2** Beta-cell antigen-specific tetramer expression in $CD4^+$ T cells corelate with disease
661 incidence in NOD mice. (**a**) Percentage of $CD4^+$ tetramer positivity T cells for three islet
662 antigens (InsB9-23, ChgA, and IAPP) (**b**) Absolute numbers of tetramer-positive $CD4^+$ T
663 cells. (**c**) Overlay of the MFI histograms by flow cytometry analysis of tetramer expression
664 in $CD4^+$ cells (**d**) Overlay representation of plasma sLAG-3 and $CD4^+$ tetramer
665 expression. (**e**) Linear regression analysis of plasma sLAG-3 levels and islet antigen-
666 specific tetramer positive $CD4^+$ T cell frequencies in $CD4^+$ T cells in NOD mice during
667 diabetic progression. Data are presented as mean ± SEM (n=10-12 in the study cohort)
668 Statistical significance was determined using one-way ANOVA with Bonferroni post-hoc
669 testing; *$p<0.05$*.

670 **Fig. 3** Antigen-specific $CD4^+$ T cell activation and immune modulation during diabetes
671 progression following adoptive transfer and immune modulation. (**a**) Schematic overview
672 of the experimental design for adoptive transfer and tracking activation of naive C6.6.9
673 TCR-Tg $CD4^+$ T cells in NOD.Scid recipient mice. (**b**) Longitudinal monitoring of blood
674 glucose levels post-transfer. (**c**) Kaplan-Meier survival analysis of diabetes onset
675 following T cell transfer. (**d**) Plasma sLAG-3 levels. (**e**) Plasma *Insulin2 (Ins2)* mRNA
676 levels measured at defined time points post-transfer. (**f-h**) Linear regression analyses
677 relating plasma sLAG-3 levels, plasma Ins2-mRNA, and blood glucose levels during
678 diabetes progression. (**i**) Frequency of circulating C6.6.9 TCR-Tg $CD4^+$ T cells in
679 peripheral blood of recipient mice over time following adoptive transfer. (**j**) Representative

680 histological images showing progressive insulitis and islet destruction in pancreatic tissue
681 from NOD.Scid recipient mice. Data are presented as mean ± SEM (n=10).

682 **Fig. 4** Longitudinal phenotypic characterization of T cell activation markers in recipients
683 following adoptive transfer. (a) Frequency of T-cell activation markers (CD25, CD69, and
684 surface LAG-3). (b) Frequency of β-cell antigen-specific tetramer-positive $CD4^+$ T cells in
685 peripheral blood over time. (c) Immunofluorescence staining of pancreatic sections on
686 days 12 and 15 post-transfer showing infiltration of ChgA, InsB9-23, and IAPP-reactive T
687 cells. (d) Quantification of immunofluorescence MFI for $ChgA^+$, $InsB9\text{-}23^+$, $IAPP^+$ cells
688 from pancreatic sections. (e, f) Percentage of different activation markers (CD25, CD69,
689 LAG-3) and β-cell antigen-specific tetramers (ChgA, InsB9-23, IAPP) expression on T
690 cells that had migrated or infiltrated into blood, pancreases and spleen at the time of
691 diabetes. All those values are represented as mean ± SEM (n=4-10). $P < 0.05$ is significant
692 and $P > 0.05$ not significant. Statistics were done by one-way ANOVA with multiple
693 comparisons, followed by the Bonferroni post hoc test.

694 **Fig. 5** Metabolic profiling and immune infiltration in the pancreas following adoptive
695 transfer of C6.6.9 T cells into NOD.Scid recipients. (**a**) Schematic overview of the
696 experimental design used to assess metabolic status and immune infiltration in the
697 pancreas after adoptive transfer. (**b**) Immunofluorescence staining of pancreatic sections
698 from control and diabetic NOD.Scid mice, showing $CD3^+$, $F4/80^+$, and $B220^+$ immune cell
699 infiltration following BDC6.9 $CD4^+$ T cell transfer. (**c, d**) Absolute number and MFI of
700 metabolic markers (CD71, CD98, and Glut-1) expressed on $CD4^+$ T cells isolated from
701 adoptively transfer NOD.Scid mice peripheral blood, pancreas, and spleen at the time of
702 diabetes onset. All data are presented as mean ± SEM (n = 4-10). Statistical significance
703 was determined using one-way ANOVA with multiple comparisons, followed by Bonferroni
704 post hoc test. $P < 0.05$ represents significant.

705 **Fig. 6.** Phenotypic characterization of TCR rearrangement in IAPP-specific $CD4^+$ T cells
706 during diabetes progression in NOD.Scid recipient mice. (a) Schematic overview of
707 experimental design for monitoring the epitope spreading following adoptive transfer of
708 C6.6.9 TCR-Tg mouse $CD4^+$ T cells into NOD.Scid recipient mice. (b) Densitometry flow

709 cytometry plot representing baseline expression status of ChgA and InsB23-9 positive on
710 C6.6.9 TCR-Tg mouse $CD4^+IAPP^+$ cells. (c) Frequency and absolute numbers of
711 $CD4^+IAPP^+ChgA^+$ and (d) $CD4^+IAPP^+InsB9\text{-}23^+$ T cells in peripheral blood over time. (e,
712 f) Frequency and absolute number of $CD4^+IAPP^+ChgA^+$ and $CD4^+IAPP^+InsB^+$ cells at the
713 time of diabetes onset were assessed in pancreas, and spleen. All values are presented
714 as mean ± SEM (n =5–6). Statistical significance was determined $P < 0.05$ represents
715 significant using one-way ANOVA with multiple comparisons, followed by the Bonferroni
716 post hoc test.

717 **Fig. 7** Longitudinal and cross-sectional analyses reveal early sLAG-3 elevation prior to
718 autoantibody expansion and clinical onset of type 1 diabetes. (a) Experimental design for
719 sample collection. Plasma was collected from healthy controls (n=28), type 1 diabetes
720 patients (n=39), and FDRs with varying numbers of autoantibodies (Ab-, n=37 Ab1+,
721 n=27; Ab2+, n=29; Ab3+, n=5). (b) Serum sLAG-3 levels in individuals with type 1
722 diabetes up to six years post-diagnosis was comparable to healthy controls, suggesting
723 that heterologous immune responses may mask earlier elevations. (c) Autoantibody-
724 negative and single-autoantibody FDRs show higher sLAG-3 levels than multiple-
725 autoantibody individuals, type 1 diabetes subjects, and controls, indicating early T cell
726 activation. (d) Experimental design for measurement of plasma sLAG-3 levels using MSD
727 U-PLEX Assays in DEWIT and Stanford Cohorts. (e, f) DEWIT longitudinal cohort show
728 higher sLAG-3 expression in females than males across both cohorts. (g) Progressor vs.
729 non-progressor trajectories in the DEWIT cohort. Progressors display a gradual increase
730 in sLAG-3 preceding diagnosis, whereas non-progressors show no change. (h, i) sLAG-
731 3 levels stratified by autoantibody category in FDRs and the general population. (j)
732 Longitudinal sLAG-3 profiling in DEWIT progressors shows a distinct peak immediately
733 before diabetes onset followed by a sharp decline after diagnosis. (k) HLA genotype
734 analysis demonstrating higher sLAG-3 expression in individuals carrying high-risk alleles.
735 Statistical significance was determined using one-way ANOVA with multiple comparisons,
736 followed by the Bonferroni post hoc test, $^*P < 0.05$ significant.

737 **Fig. 8** sLAG-3 as an early and sensitive marker of T cell activation during vaccination and
738 viral infection C57BL/6 Mice. (a) Schematic illustration of before and 10 days after

739 COVID-19 vaccination, indicating rapid T-cell activation preceding antibody development.
740 (b) Normalized protein expression (NPX) of sLAG-3 over time in before and after 10 days
741 of Covid vaccination from plasma. Each donors' samples are connected by a line. (c)
742 Schematic representation of time-course analysis of plasma analytes in-vivo CVB-
743 infected C57BL/6 mice. (d) Plasma sLAG-3 levels form C57BL/6 mice infected with CVB.
744 (e) Plasma IFN-γ concentrations increase after infection, with a marked rise at day 6,
745 reflecting concurrent immune activation. (f, g) Flow cytometry reveals time-dependent
746 increases in IFN-γ-producing $CD4^+$ and $CD8^+$ T cells in peripheral blood following CVB
747 infection. (h, I) Expression of T cell activation markers CD25 and CD69. All values are
748 presented as mean ± SEM (n=8). Statistical significance was determined using one-way
749 ANOVA, followed by the Bonferroni post hoc test. *$P < 0.05$ represent significant.

750

References

[1] Atkinson MA, Mirmira RG (2023) The pathogenic "symphony" in type 1 diabetes: A disorder of the immune system, beta cells, and exocrine pancreas. Cell Metab 35(9): 1500-1518. 10.1016/j.cmet.2023.06.018

[2] Burrack AL, Martinov T, Fife BT (2017) T Cell-Mediated Beta Cell Destruction: Autoimmunity and Alloimmunity in the Context of Type 1 Diabetes. Front Endocrinol (Lausanne) 8: 343. 10.3389/fendo.2017.00343

[3] Houeiss P, Luce S, Boitard C (2022) Environmental Triggering of Type 1 Diabetes Autoimmunity. Front Endocrinol (Lausanne) 13: 933965. 10.3389/fendo.2022.933965

[4] Roy S, Pokharel P, Piganelli JD (2024) Decoding the immune dance: Unraveling the interplay between beta cells and type 1 diabetes. Mol Metab 88: 101998. 10.1016/j.molmet.2024.101998

[5] Maahs DM, West NA, Lawrence JM, Mayer-Davis EJ (2010) Epidemiology of type 1 diabetes. Endocrinol Metab Clin North Am 39(3): 481-497. 10.1016/j.ecl.2010.05.011

[6] Group DP (2006) Incidence and trends of childhood Type 1 diabetes worldwide 1990-1999. Diabet Med 23(8): 857-866. 10.1111/j.1464-5491.2006.01925.x

[7] Popoviciu MS, Kaka N, Sethi Y, Patel N, Chopra H, Cavalu S (2023) Type 1 Diabetes Mellitus and Autoimmune Diseases: A Critical Review of the Association and the Application of Personalized Medicine. J Pers Med 13(3). 10.3390/jpm13030422

[8] Mallone R, Bismuth E, Thivolet C, et al. (2025) Screening and care for preclinical stage 1-2 type 1 diabetes in first-degree relatives: French expert position statement. Diabetes Metab 51(1): 101603. 10.1016/j.diabet.2024.101603

[9] Steck AK, Rewers MJ (2011) Genetics of type 1 diabetes. Clin Chem 57(2): 176-185. 10.1373/clinchem.2010.148221

[10] Thakkar S, Chopra A, Nagendra L, Kalra S, Bhattacharya S (2023) Teplizumab in Type 1 Diabetes Mellitus: An Updated Review. touchREV Endocrinol 19(2): 22-30. 10.17925/EE.2023.19.2.7

[11] Kokori E, Olatunji G, Ogieuhi IJ, et al. (2024) Teplizumab's immunomodulatory effects on pancreatic beta-cell function in type 1 diabetes mellitus. Clin Diabetes Endocrinol 10(1): 23. 10.1186/s40842-024-00181-w

[12] Li N, Wang Y, Forbes K, et al. (2007) Metalloproteases regulate T-cell proliferation and effector function via LAG-3. EMBO J 26(2): 494-504. 10.1038/sj.emboj.7601520

[13] Scherm MG, Wyatt RC, Serr I, Anz D, Richardson SJ, Daniel C (2022) Beta cell and immune cell interactions in autoimmune type 1 diabetes: How they meet and talk to each other. Mol Metab 64: 101565. 10.1016/j.molmet.2022.101565

[14] Andrews LP, Marciscano AE, Drake CG, Vignali DA (2017) LAG3 (CD223) as a cancer immunotherapy target. Immunological reviews 276(1): 80-96. 10.1111/imr.12519

[15] Anderson MS, Bluestone JA (2005) The NOD mouse: a model of immune dysregulation. Annu Rev Immunol 23: 447-485. 10.1146/annurev.immunol.23.021704.115643

[16] Cieplińska K, Niedziela E, Jagielska E, Pałyga I, Słuszniak A, Kowalska A (2025) Elevated Levels of sLAG-3 as a Possible Biomarker in Graves' Disease With and Without

Thyroid Eye Disease: A Prospective Observational Case-Control Study. Medicina (Kaunas) 61(9). 10.3390/medicina61091664

[17] Anderson Ana C, Joller N, Kuchroo Vijay K (2016) Lag-3, Tim-3, and TIGIT: Co-inhibitory Receptors with Specialized Functions in Immune Regulation. Immunity 44(5): 989-1004. 10.1016/j.immuni.2016.05.001

[18] Ruffo E, Wu RC, Bruno TC, Workman CJ, Vignali DAA (2019) Lymphocyte-activation gene 3 (LAG3): The next immune checkpoint receptor. Semin Immunol 42: 101305. 10.1016/j.smim.2019.101305

[19] Botticelli A, Zizzari IG, Scagnoli S, et al. (2021) The Role of Soluble LAG3 and Soluble Immune Checkpoints Profile in Advanced Head and Neck Cancer: A Pilot Study. J Pers Med 11(7). 10.3390/jpm11070651

[20] SYED F, MAIER BF, ANDERSON-BAUCUM E, MASTRACCI TL, EVANS-MOLINA C, MIRMIRA R (2020) 82-OR: Exosomes from Human ß-Cells Incorporate Stress Granule Components and May Serve as Biomarkers of ß-Cell Stress in Type 1 Diabetes. Diabetes 69(Supplement_1). 10.2337/db20-82-OR

[21] Dekkers MC, Lambooij JM, Pu X, et al. (2024) Extracellular vesicles derived from stressed beta cells mediate monocyte activation and contribute to islet inflammation. Front Immunol 15: 1393248. 10.3389/fimmu.2024.1393248

[22] Dekkers MC, Pu X, Enciso-Martinez A, Zaldumbide A (2024) Beta-Cell-Derived Extracellular Vesicles: Mediators of Intercellular Communication in the Islet Microenvironment in Type 1 Diabetes. Cells 13(23). 10.3390/cells13231996

[23] Kracht MJ, van Lummel M, Nikolic T, et al. (2017) Autoimmunity against a defective ribosomal insulin gene product in type 1 diabetes. Nat Med 23(4): 501-507. 10.1038/nm.4289

[24] van Tienhoven R, Jansen D, Park M, et al. (2024) Induction of islet autoimmunity to defective ribosomal product of the insulin gene as neoantigen after anti-cancer immunotherapy leading to autoimmune diabetes. Front Immunol 15: 1384406. 10.3389/fimmu.2024.1384406

[25] van Tienhoven R, O'Meally D, Scott TA, et al. (2025) Genetic protection from type 1 diabetes resulting from accelerated insulin mRNA decay. Cell 188(9): 2407-2416 e2409. 10.1016/j.cell.2025.02.018

[26] Anand V, Li Y, Liu B, et al. (2021) Islet Autoimmunity and HLA Markers of Presymptomatic and Clinical Type 1 Diabetes: Joint Analyses of Prospective Cohort Studies in Finland, Germany, Sweden, and the U.S. Diabetes Care 44(10): 2269-2276. 10.2337/dc20-1836

[27] Gong Q, Sharma M, Kuan EL, et al. (2024) Longitudinal Multi-omic Immune Profiling Reveals Age-Related Immune Cell Dynamics in Healthy Adults. bioRxiv. 10.1101/2024.09.10.612119

[28] Aggarwal V, Workman CJ, Vignali DAA (2023) LAG-3 as the third checkpoint inhibitor. Nature Immunology 24(9): 1415-1422. 10.1038/s41590-023-01569-z

[29] Camisaschi C, Casati C, Rini F, et al. (2010) LAG-3 expression defines a subset of CD4(+)CD25(high)Foxp3(+) regulatory T cells that are expanded at tumor sites. J Immunol 184(11): 6545-6551. 10.4049/jimmunol.0903879

[30] Marré ML, Profozich JL, Coneybeer JT, et al. (2016) Inherent ER stress in pancreatic islet β cells causes self-recognition by autoreactive T cells in type 1 diabetes. J Autoimmun 72: 33-46. 10.1016/j.jaut.2016.04.009

[31] Catrina AM, Popa MA, Văcaru AM, Fenyo IM (2021) Inflammatory status of the pancreas in NOD mice that do not develop overt diabetes. Rom J Morphol Embryol 62(1): 109-115. 10.47162/rjme.62.1.10

[32] Piganelli JD, Flores SC, Cruz C, et al. (2002) A Metalloporphyrin-Based Superoxide Dismutase Mimic Inhibits Adoptive Transfer of Autoimmune Diabetes by a Diabetogenic T-Cell Clone. Diabetes 51(2): 347-355. 10.2337/diabetes.51.2.347

[33] Mitchell JS, Spanier JA, Dwyer AJ, et al. (2024) CD4+ T cells reactive to a hybrid peptide from insulin-chromogranin A adopt a distinct effector fate and are pathogenic in autoimmune diabetes. Immunity 57(10): 2399-2415.e2398. https://doi.org/10.1016/j.immuni.2024.07.024

[34] Bettini M, Vignali DA (2011) T cell-driven initiation and propagation of autoimmune diabetes. Curr Opin Immunol 23(6): 754-760. 10.1016/j.coi.2011.10.002

[35] Clark M, Kroger CJ, Ke Q, Tisch RM (2020) The Role of T Cell Receptor Signaling in the Development of Type 1 Diabetes. Front Immunol 11: 615371. 10.3389/fimmu.2020.615371

[36] Hussain S, Delovitch TL (2005) Dysregulated B7-1 and B7-2 expression on nonobese diabetic mouse B cells is associated with increased T cell costimulation and the development of insulitis. J Immunol 174(2): 680-687. 10.4049/jimmunol.174.2.680

[37] Tian J, Zekzer D, Hanssen L, Lu Y, Olcott A, Kaufman DL (2001) Lipopolysaccharide-activated B cells down-regulate Th1 immunity and prevent autoimmune diabetes in nonobese diabetic mice. J Immunol 167(2): 1081-1089. 10.4049/jimmunol.167.2.1081

[38] Qi Q, Cavanagh MM, Le Saux S, et al. (2016) Diversification of the antigen-specific T cell receptor repertoire after varicella zoster vaccination. Sci Transl Med 8(332): 332ra346. 10.1126/scitranslmed.aaf1725

[39] Straub A, Grassmann S, Jarosch S, et al. (2023) Recruitment of epitope-specific T cell clones with a low-avidity threshold supports efficacy against mutational escape upon re-infection. Immunity 56(6): 1269-1284.e1266. https://doi.org/10.1016/j.immuni.2023.04.010

[40] Yi J, Miller AT, Archambault AS, et al. (2022) Antigen-specific depletion of CD4(+) T cells by CAR T cells reveals distinct roles of higher- and lower-affinity TCRs during autoimmunity. Sci Immunol 7(76): eabo0777. 10.1126/sciimmunol.abo0777

[41] Ize-Ludlow D, Lightfoot YL, Parker M, et al. (2011) Progressive erosion of β-cell function precedes the onset of hyperglycemia in the NOD mouse model of type 1 diabetes. Diabetes 60(8): 2086-2091. 10.2337/db11-0373

[42] Syed F, Krishnan P, Chang G, et al. (2023) beta Cell microRNAs Function as Molecular Hubs of Type 1 Diabetes Pathogenesis and as Biomarkers of Diabetes Risk. bioRxiv. 10.1101/2023.06.15.545170

[43] Guerrero JA, Klysz DD, Chen Y, et al. (2024) GLUT1 overexpression in CAR-T cells induces metabolic reprogramming and enhances potency. Nat Commun 15(1): 8658. 10.1038/s41467-024-52666-y

879 [44] Poznanski SM, Singh K, Ritchie TM, et al. (2021) Metabolic flexibility determines
880 human NK cell functional fate in the tumor microenvironment. Cell Metab 33(6): 1205-
881 1220 e1205. 10.1016/j.cmet.2021.03.023
882 [45] Salzberger W, Martrus G, Bachmann K, et al. (2018) Tissue-resident NK cells differ in
883 their expression profile of the nutrient transporters Glut1, CD98 and CD71. PLoS One
884 13(7): e0201170. 10.1371/journal.pone.0201170
885 [46] Jessop MK (1990) Homoeopathy. Vet Rec 126(20): 514
886 [47] Delmastro-Greenwood M, Hughan KS, Vitturi DA, et al. (2015) Nitrite and nitrate-
887 dependent generation of anti-inflammatory fatty acid nitroalkenes. Free Radical Biology
888 and Medicine 89: 333-341. https://doi.org/10.1016/j.freeradbiomed.2015.07.149
889 [48] Previte DM, Martins CP, O'Connor EC, et al. (2019) Lymphocyte Activation Gene-3
890 Maintains Mitochondrial and Metabolic Quiescence in Naive CD4(+) T Cells. Cell Rep
891 27(1): 129-141.e124. 10.1016/j.celrep.2019.03.004
892 [49] Previte DM, O'Connor EC, Novak EA, Martins CP, Mollen KP, Piganelli JD (2017)
893 Reactive oxygen species are required for driving efficient and sustained aerobic
894 glycolysis during CD4+ T cell activation. PLoS One 12(4): e0175549.
895 10.1371/journal.pone.0175549
896 [50] Sartoris S, Del Pozzo G (2024) Exploring the HLA complex in autoimmunity: From the
897 risk haplotypes to the modulation of expression. Clinical Immunology 265: 110266.
898 https://doi.org/10.1016/j.clim.2024.110266
899 [51] Sartoris S, Del Pozzo G (2024) Exploring the HLA complex in autoimmunity: From the
900 risk haplotypes to the modulation of expression. Clin Immunol 265: 110266.
901 10.1016/j.clim.2024.110266

902

903

Fig. 1

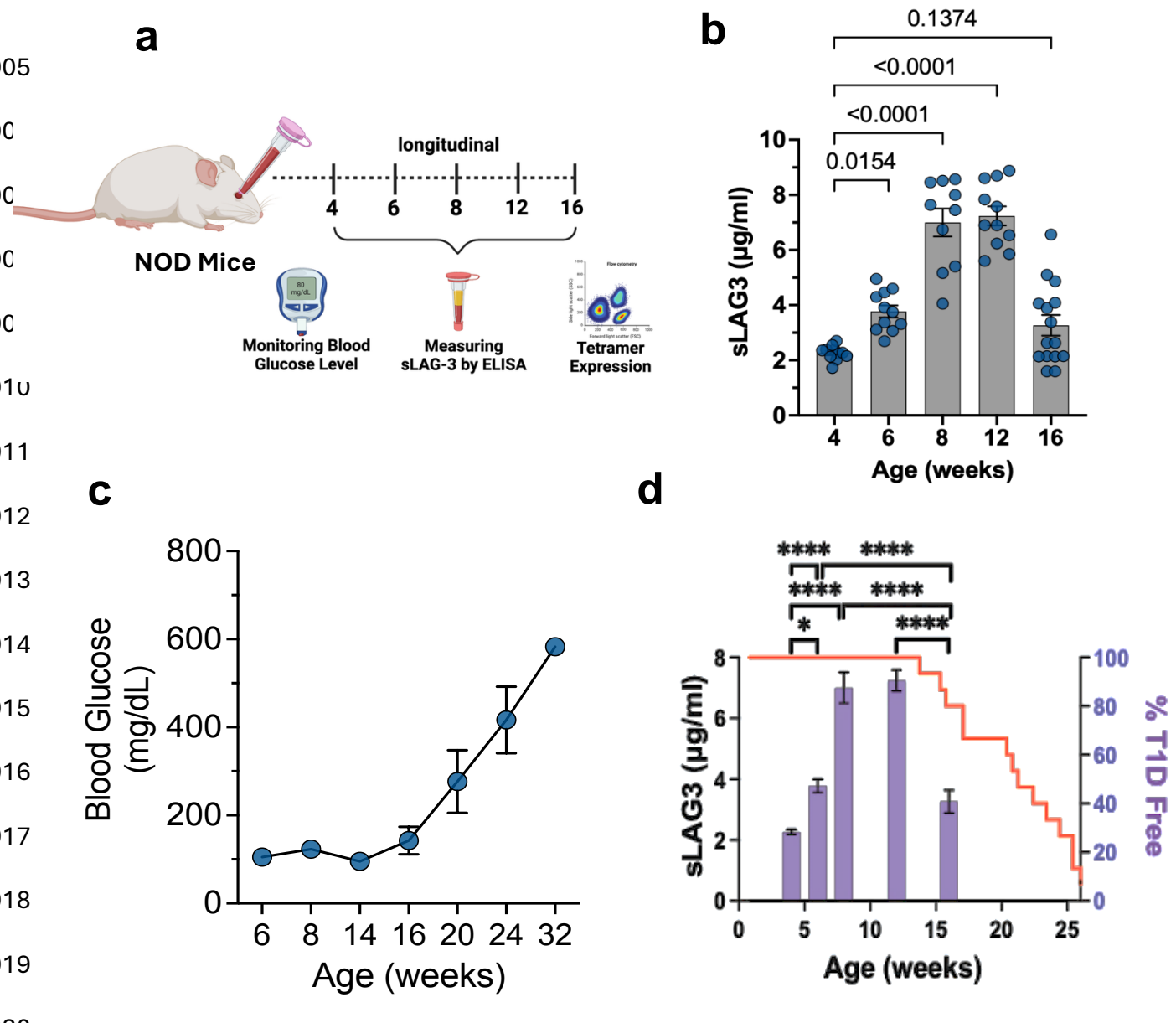
a
longitudinal
4
6
8
12
16
NOD Mice
Monitoring Blood Glucose Level
Measuring sLAG-3 by ELISA
Tetramer Expression
b
0.1374
<0.0001
<0.0001
0.0154
sLAG3 (µg/ml)
Age (weeks)
c
Blood Glucose (mg/dL)
Age (weeks)
d
****
****
****
****
*
****
sLAG3 (µg/ml)
% T1D Free
Age (weeks)

Fig. 2

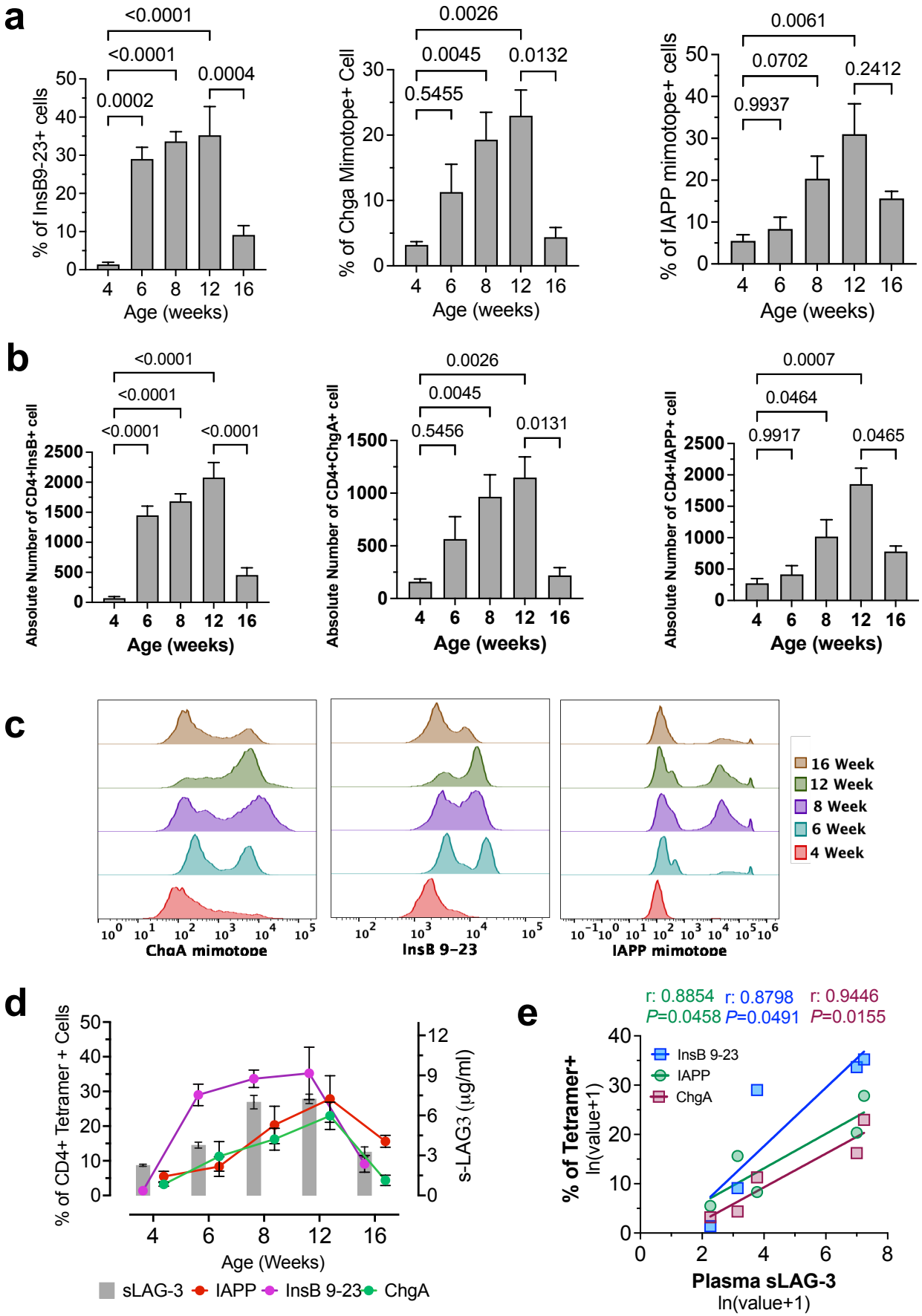
a
<0.0001
<0.0001
0.0002
0.0004
% of InsB9-23+ cells
Age (weeks)
0.0026
0.0045
0.5455
0.0132
% of Chga Mimotope+ Cell
Age (weeks)
0.0061
0.0702
0.9937
0.2412
% of IAPP mimotope+ cells
Age (weeks)
b
<0.0001
<0.0001
<0.0001
<0.0001
Absolute Number of CD4+InsB+ cell
Age (weeks)
0.0026
0.0045
0.5456
0.0131
Absolute Number of CD4+ChgA+ cell
Age (weeks)
0.0007
0.0464
0.9917
0.0465
Absolute Number of CD4+IAPP+ cell
Age (weeks)
c
16 Week
12 Week
8 Week
6 Week
4 Week
ChgA mimotope
InsB 9-23
IAPP mimotope
d
% of CD4+ Tetramer + Cells
s-LAG3 (μg/ml)
Age (Weeks)
sLAG-3
IAPP
InsB 9-23
ChgA
e
r: 0.8854 r: 0.8798 r: 0.9446
P=0.0458 P=0.0491 P=0.0155
InsB 9-23
IAPP
ChgA
% of Tetramer+
ln(value+1)
Plasma sLAG-3
ln(value+1)

Fig. 3

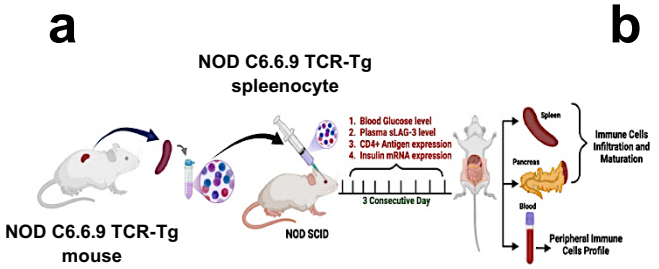
a
NOD C6.6.9 TCR-Tg spleenocyte
NOD C6.6.9 TCR-Tg mouse
NOD SCID
1. Blood Glucose level
2. Plasma sLAG-3 level
3. CD4+ Antigen expression
4. Insulin mRNA expression
3 Consecutive Day
Spleen
Pancreas
Blood
Immune Cells Infiltration and Maturation
Peripheral Immune Cells Profile

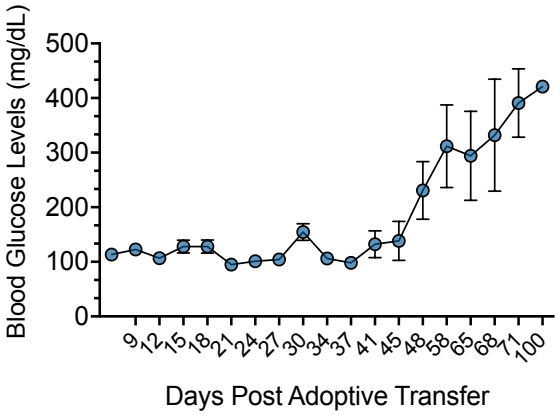
b
Blood Glucose Levels (mg/dL)
Days Post Adoptive Transfer

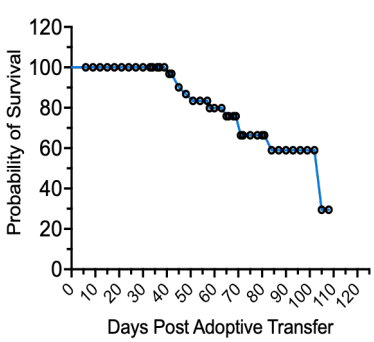
c
Probability of Survival
Days Post Adoptive Transfer

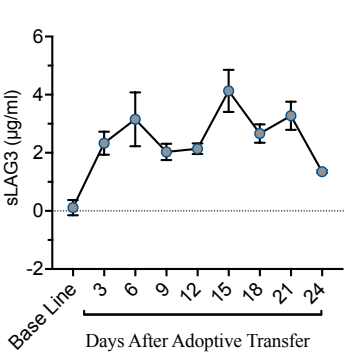
d
sLAG3 (μg/ml)
Base Line
Days After Adoptive Transfer

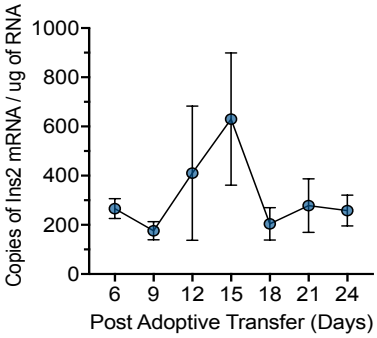
e
Copies of Ins2 mRNA / ug of RNA
Post Adoptive Transfer (Days)

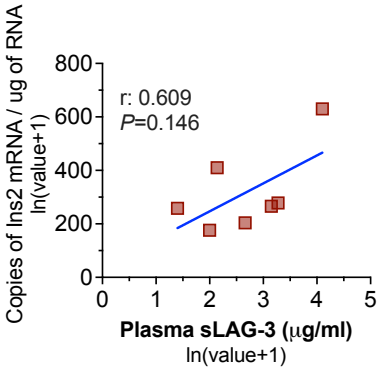
f
Copies of Ins2 mRNA / ug of RNA ln(value+1)
r: 0.609
P=0.146
Plasma sLAG-3 (μg/ml) ln(value+1)

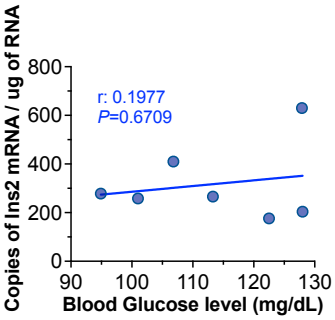
g
Copies of Ins2 mRNA / ug of RNA
r: 0.1977
P=0.6709
Blood Glucose level (mg/dL)

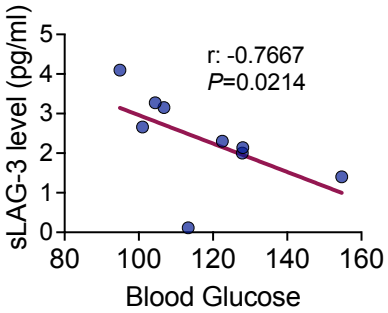
h
sLAG-3 level (pg/ml)
r: -0.7667
P=0.0214
Blood Glucose

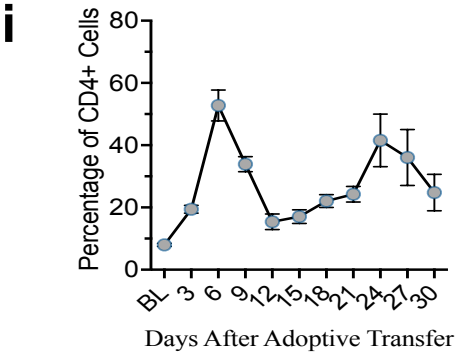
i
Percentage of CD4+ Cells
Days After Adoptive Transfer

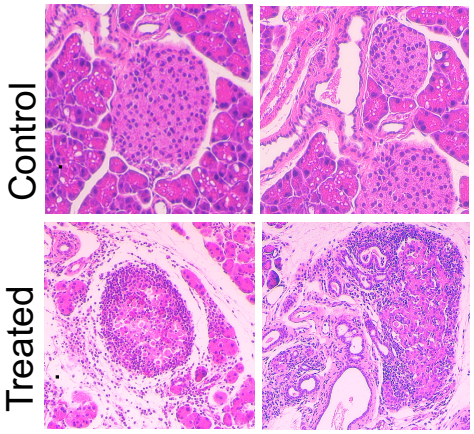
j
Control
Treated

Fig. 4

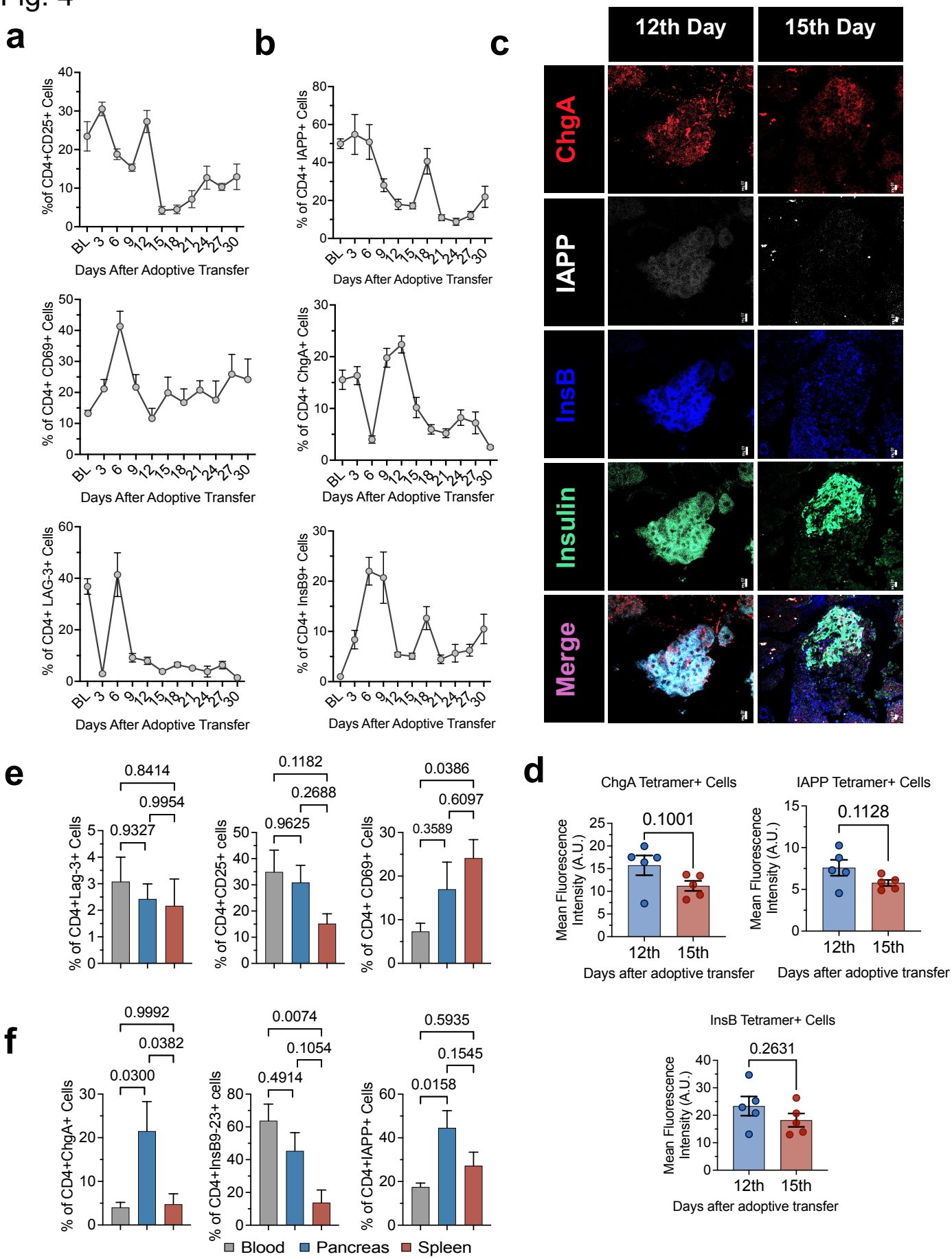
a
b
c
12th Day
15th Day
ChgA
IAPP
InsB
Insulin
Merge
%of CD4+CD25+ Cells
% of CD4+ IAPP+ Cells
% of CD4+ CD69+ Cells
% of CD4+ ChgA+ Cells
% of CD4+ LAG-3+ Cells
% of CD4+ InsB9+ Cells
BL 3 6 9 12 15 18 21 24 27 30
Days After Adoptive Transfer
e
0.8414
0.9954
0.9327
% of CD4+Lag-3+ Cells
0.1182
0.2688
0.9625
% of CD4+CD25+ cells
0.0386
0.6097
0.3589
% of CD4+ CD69+ Cells
d
ChgA Tetramer+ Cells
0.1001
Mean Fluorescence Intensity (A.U.)
12th 15th
Days after adoptive transfer
IAPP Tetramer+ Cells
0.1128
Mean Fluorescence Intensity (A.U.)
12th 15th
Days after adoptive transfer
f
0.9992
0.0382
0.0300
% of CD4+ChgA+ Cells
0.0074
0.1054
0.4914
% of CD4+InsB9-23+ cells
0.5935
0.1545
0.0158
% of CD4+IAPP+ Cells
Blood
Pancreas
Spleen
InsB Tetramer+ Cells
0.2631
Mean Fluorescence Intensity (A.U.)
12th 15th
Days after adoptive transfer

Fig. 5

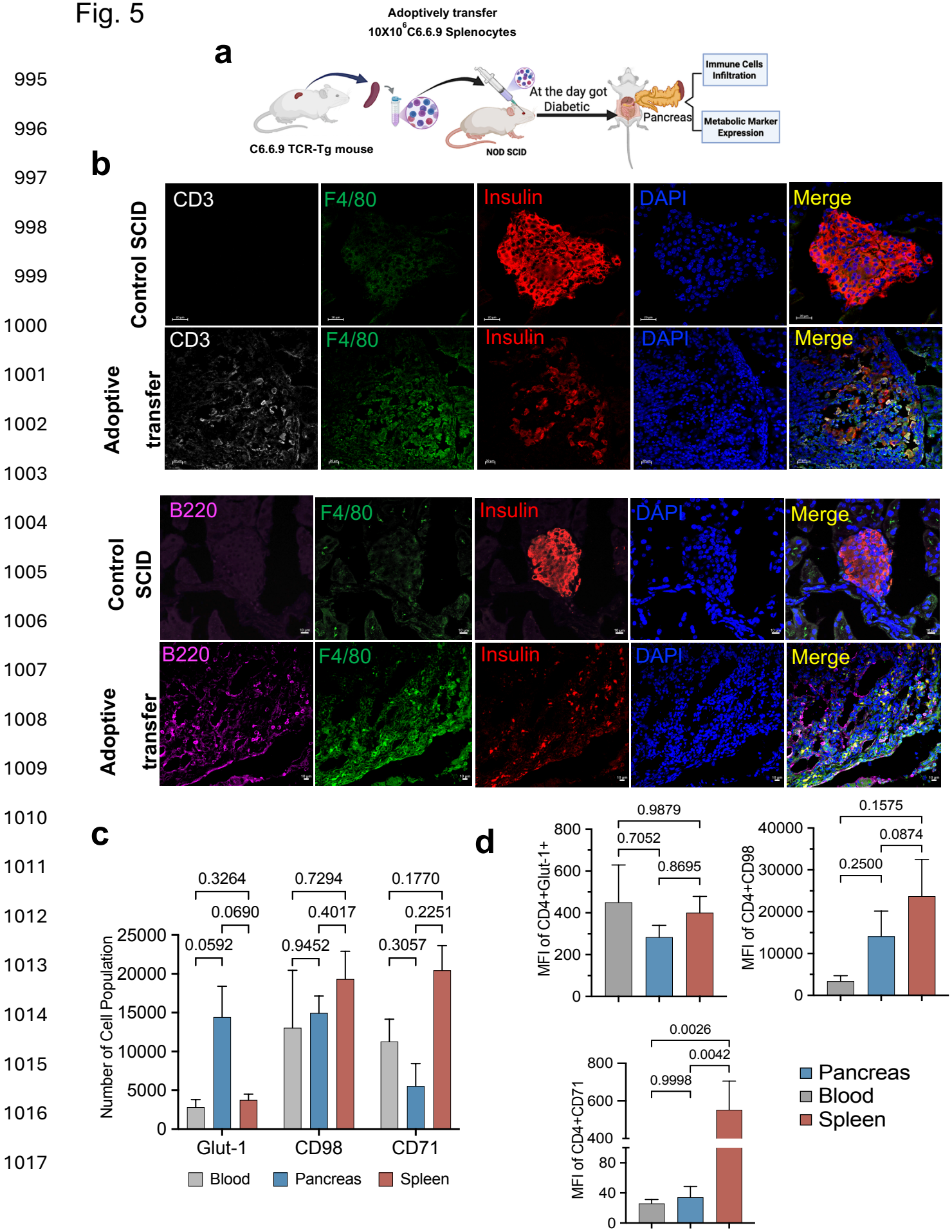
a
Adoptively transfer
10X10^6 C6.6.9 Splenocytes
C6.6.9 TCR-Tg mouse
NOD SCID
At the day got Diabetic
Pancreas
Immune Cells Infiltration
Metabolic Marker Expression
b
Control SCID
Adoptive transfer
CD3
F4/80
Insulin
DAPI
Merge
B220
c
Number of Cell Population
0.3264
0.0690
0.0592
0.7294
0.4017
0.9452
0.1770
0.2251
0.3057
Glut-1
CD98
CD71
Blood
Pancreas
Spleen
d
MFI of CD4+Glut-1+
0.9879
0.7052
0.8695
MFI of CD4+CD98
0.1575
0.0874
0.2500
MFI of CD4+CD71
0.0026
0.0042
0.9998
Pancreas
Blood
Spleen

Fig. 6

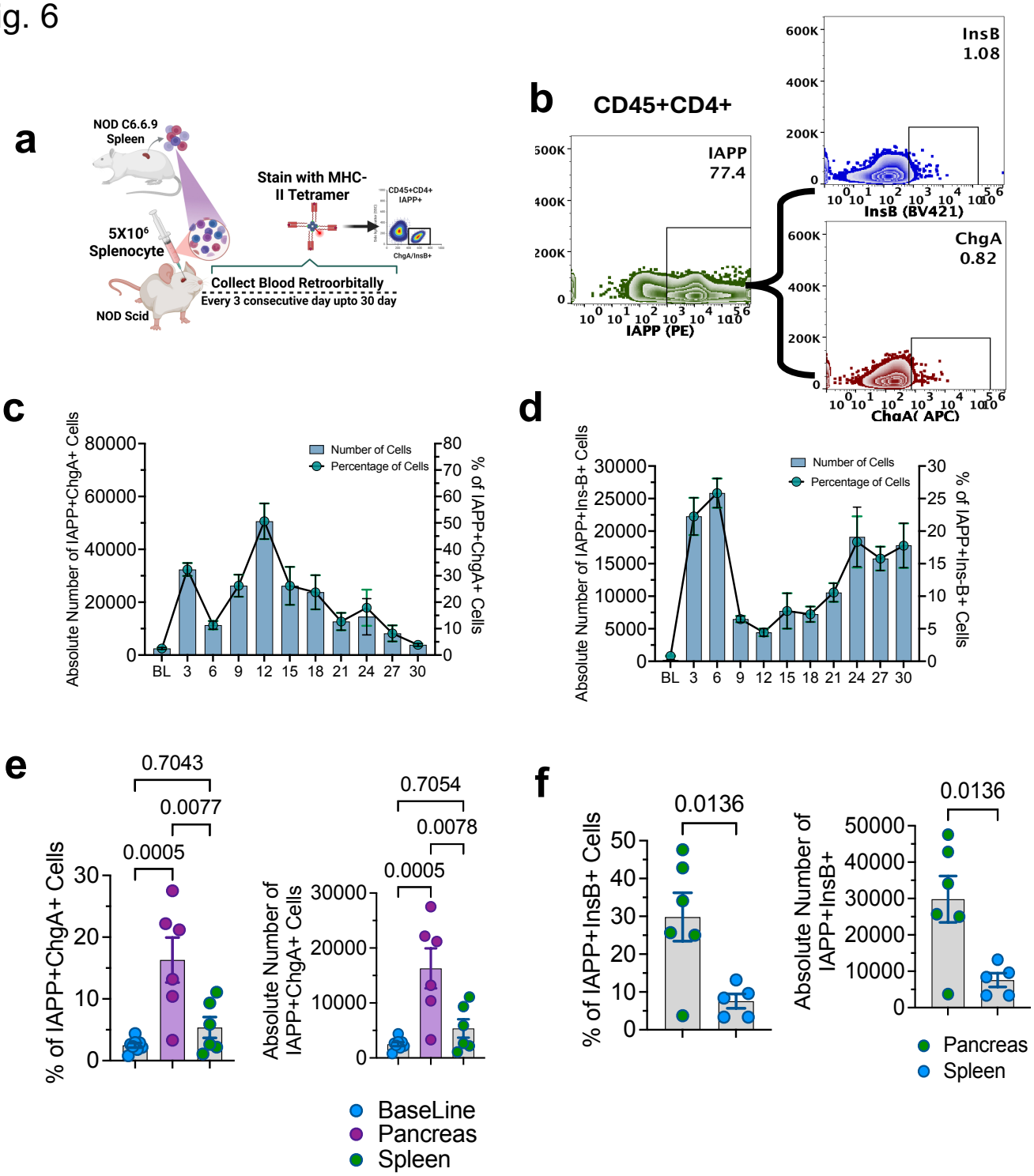
a
NOD C6.6.9 Spleen
Stain with MHC-II Tetramer
5X10⁶ Splenocyte
NOD Scid
Collect Blood Retroorbitally
Every 3 consecutive day upto 30 day
b
CD45+CD4+
IAPP 77.4
IAPP (PE)
InsB 1.08
InsB (BV421)
ChgA 0.82
ChgA(APC)
c
Absolute Number of IAPP+ChgA+ Cells
% of IAPP+ChgA+ Cells
Number of Cells
Percentage of Cells
BL 3 6 9 12 15 18 21 24 27 30
d
Absolute Number of IAPP+Ins-B+ Cells
% of IAPP+Ins-B+ Cells
Number of Cells
Percentage of Cells
e
% of IAPP+ChgA+ Cells
0.7043
0.0077
0.0005
Absolute Number of IAPP+ChgA+ Cells
0.7054
0.0078
0.0005
BaseLine
Pancreas
Spleen
f
% of IAPP+InsB+ Cells
0.0136
Absolute Number of IAPP+InsB+
0.0136
Pancreas
Spleen

Fig. 7

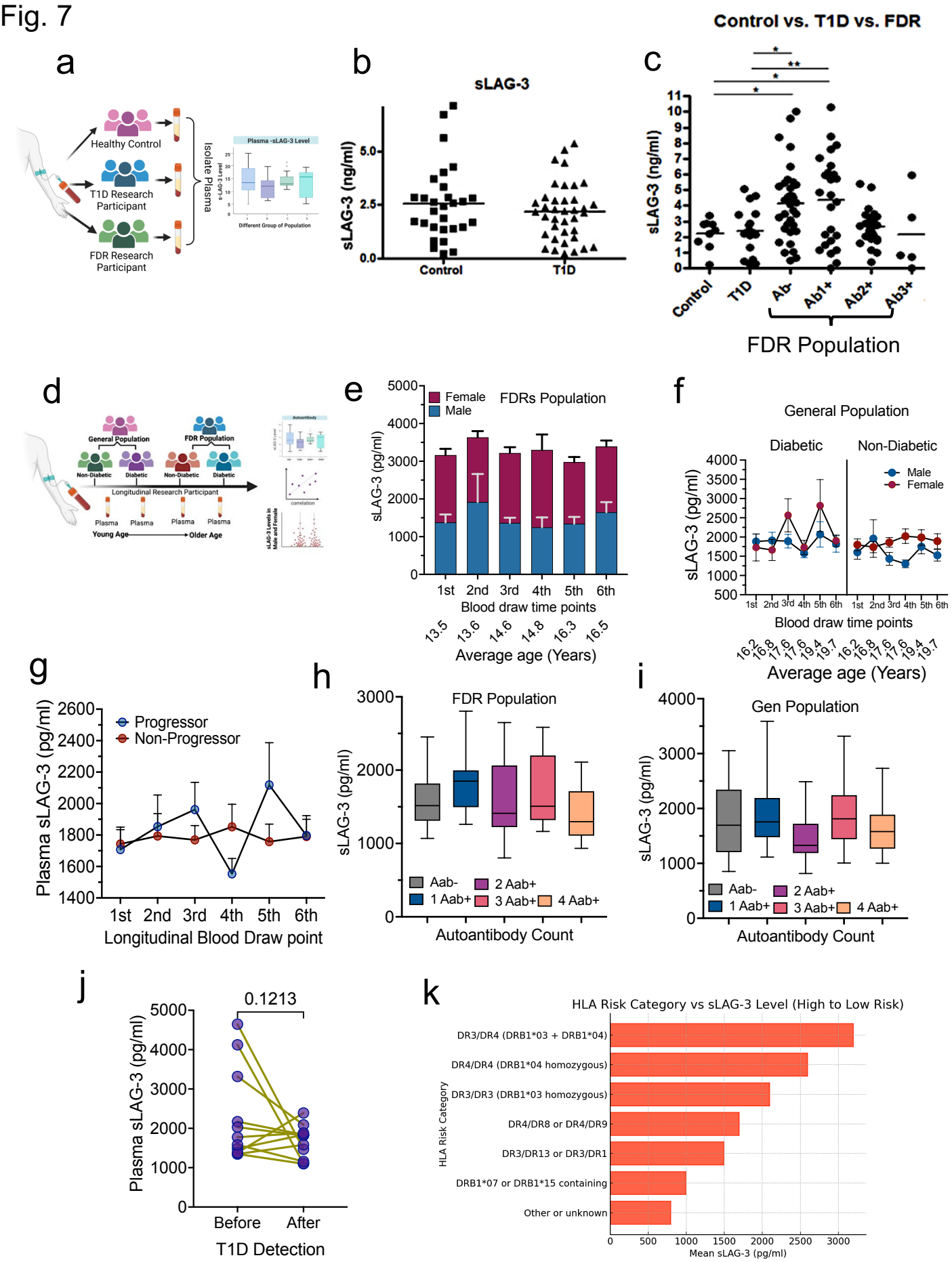
a
Healthy Control
T1D Research Participant
FDR Research Participant
Isolate Plasma
Plasma -sLAG-3 Level
Different Group of Population
b
sLAG-3
sLAG-3 (ng/ml)
Control
T1D
c
Control vs. T1D vs. FDR
sLAG-3 (ng/ml)
Control
T1D
Ab-
Ab1+
Ab2+
Ab3+
FDR Population
d
General Population
FDR Population
Non-Diabetic
Diabetic
Longitudinal Research Participant
Plasma
Young Age
Older Age
e
Female
Male
FDRs Population
sLAG-3 (pg/ml)
1st
2nd
3rd
4th
5th
6th
Blood draw time points
13.5
13.6
14.6
14.8
16.3
16.5
Average age (Years)
f
General Population
Diabetic
Non-Diabetic
Male
Female
sLAG-3 (pg/ml)
Blood draw time points
Average age (Years)
g
Progressor
Non-Progressor
Plasma sLAG-3 (pg/ml)
Longitudinal Blood Draw point
h
FDR Population
sLAG-3 (pg/ml)
Aab-
1 Aab+
2 Aab+
3 Aab+
4 Aab+
Autoantibody Count
i
Gen Population
sLAG-3 (pg/ml)
Aab-
1 Aab+
2 Aab+
3 Aab+
4 Aab+
Autoantibody Count
j
0.1213
Plasma sLAG-3 (pg/ml)
Before
After
T1D Detection
k
HLA Risk Category vs sLAG-3 Level (High to Low Risk)
DR3/DR4 (DRB1*03 + DRB1*04)
DR4/DR4 (DRB1*04 homozygous)
DR3/DR3 (DRB1*03 homozygous)
DR4/DR8 or DR4/DR9
DR3/DR13 or DR3/DR1
DRB1*07 or DRB1*15 containing
Other or unknown
HLA Risk Category
Mean sLAG-3 (pg/ml)

Fig. 8

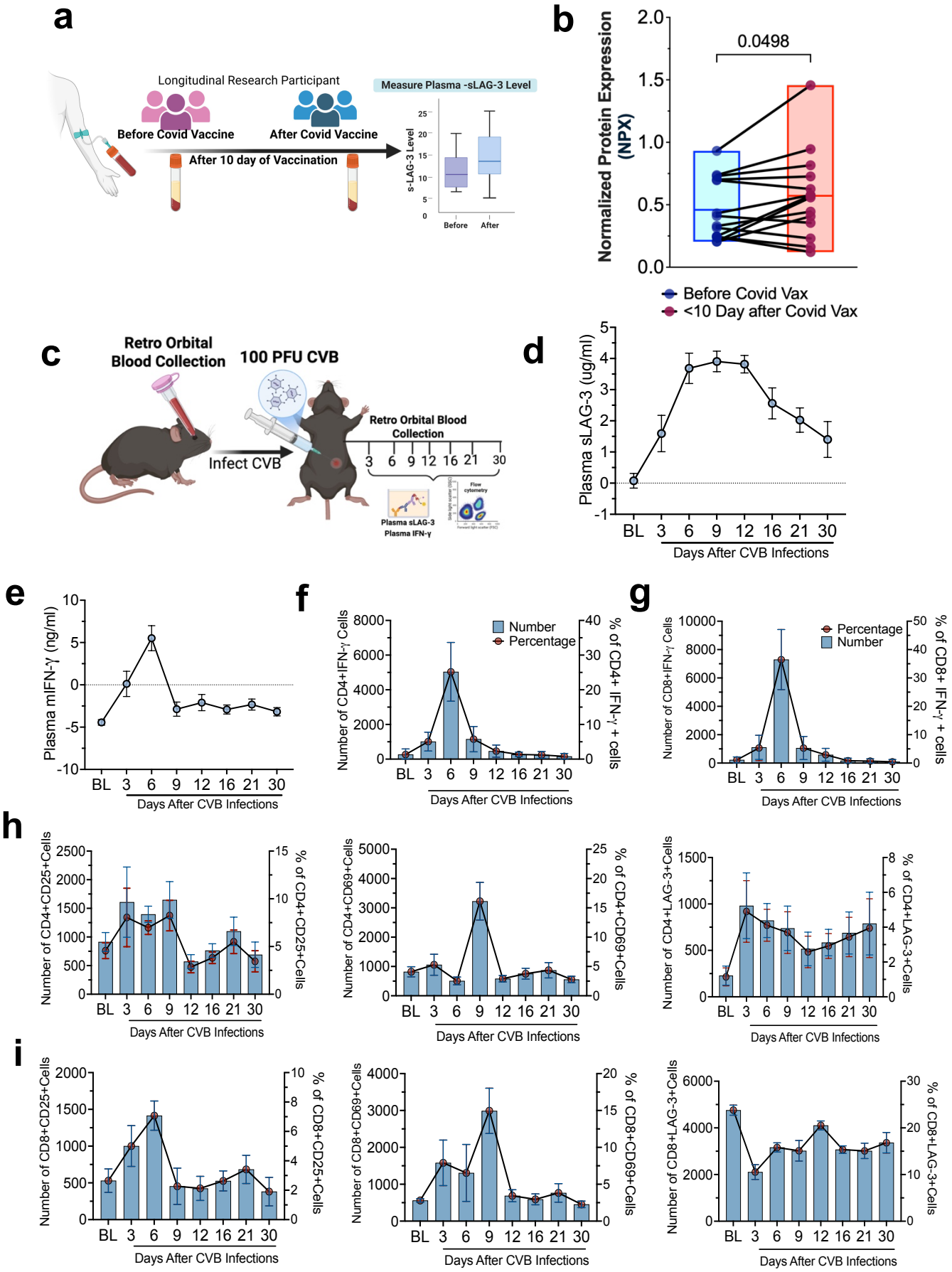
a
Longitudinal Research Participant
Before Covid Vaccine
After Covid Vaccine
After 10 day of Vaccination
Measure Plasma -sLAG-3 Level
s-LAG-3 Level
Before
After
b
Normalized Protein Expression (NPX)
0.0498
Before Covid Vax
<10 Day after Covid Vax
c
Retro Orbital Blood Collection
100 PFU CVB
Infect CVB
Retro Orbital Blood Collection
3 6 9 12 16 21 30
Plasma sLAG-3
Plasma IFN-γ
Flow cytometry
d
Plasma sLAG-3 (ug/ml)
BL 3 6 9 12 16 21 30
Days After CVB Infections
e
Plasma mIFN-γ (ng/ml)
Days After CVB Infections
f
Number of CD4+IFN-γ Cells
% of CD4+ IFN-γ + cells
Number
Percentage
Days After CVB Infections
g
Number of CD8+IFN-γ Cells
% of CD8+ IFN-γ + cells
Percentage
Number
Days After CVB Infections
h
Number of CD4+CD25+Cells
% of CD4+CD25+Cells
Number of CD4+CD69+Cells
% of CD4+CD69+Cells
Number of CD4+LAG-3+Cells
% of CD4+LAG-3+Cells
Days After CVB Infections
i
Number of CD8+CD25+Cells
% of CD8+CD25+Cells
Number of CD8+CD69+Cells
% of CD8+CD69+Cells
Number of CD8+LAG-3+Cells
% of CD8+LAG-3+Cells
Days After CVB Infections